Systematic Entomology

Systematic Entomology (2021), **46**, 526–557 DOI: 10.1111/syen.12474

Morphological phylogeny of Panorpidae (Mecoptera: Panorpoidea)

JI-SHEN WANG[1,2] and BAO-ZHEN HUA[1]

[1]Key Laboratory of Plant Protection Resources and Pest Management, Ministry of Education, Entomological Museum, College of Plant Protection, Northwest A&F University, Yangling, Shaanxi, 712100, China and [2]College of Agriculture and Biological Sciences, Dali University, Dali, Yunnan, 671003, China

Abstract. Panorpidae is the largest family of Mecoptera with approximately 500 described species in one extinct and eight extant genera. The phylogeny of Panorpidae was inferred from DNA sequences recently, but has not been comprehensively studied based on morphological characters to date. Here, the phylogeny of Panorpidae was analysed for 155 extant species in eight genera based on 182 morphological characters of adults under Maximum Parsimony and Maximum Likelihood, respectively, with two species of Choristidae and three species of Panorpodidae as outgroups. The resulting phylogenetic trees are overall consistent with those reconstructed in the molecular analyses, and support the monophyly of two major clades and all the extant genera except *Panorpa* and *Neopanorpa*, which may need further splitting. A new subfamily, Neopanorpinae **subfam.n.**, is established to include *Neopanorpa* and *Leptopanorpa*, with all the other genera assigned to Panorpinae. Thirty-two species groups (24 in *Panorpa* and eight in *Neopanorpa*) are recognized. We speculate that Panorpidae likely originated from East Asia, with independent dispersal events that probably occurred at least twice for the Indonesian fauna, five times for the Japanese fauna, twice for the western Palearctic fauna, and four times for the Nearctic fauna.
This work has been registered in ZooBank: http://zoobank.org/urn:lsid:zoobank.org:pub:7B451D1E-1DA3-4D65-B6BD-4730B10416E5

Introduction

Mecoptera is a small relict order of holometabolous insects, and constitutes the superorder Antliophora ('pump-bearers') together with Diptera and Siphonaptera (Grimaldi & Engel, 2005), although the sperm pump is regarded as independently derived between Mecoptera + Siphonaptera and Diptera (Hünefeld & Beutel, 2005; Mickoleit, 2008; Boudinot, 2018). Mecoptera likely originated in the Early Permian (Novokshonov, 2004) and contains more than 700 extinct species in ca. 210 genera and 40 families (Lin *et al.*, 2019; Soszyńska-Maj *et al.*, 2020). However, only nine families have survived to the present day, including approximately 800 extant species in ca. 40 genera (Wang & Hua, 2017, 2018, 2019a,b, 2020; Bicha, 2018).

Based on morphological and molecular evidence, the extinct families †Mesochoristidae and †Permopanorpidae and the extant Nannochoristidae and Boreidae should possibly be removed from Mecoptera (Willmann, 1987, 1989; Whiting, 2002; Beutel & Baum, 2008; Beutel & Friedrich, 2019). In this case, only the remaining families in the monophyletic group Pistillifera are left in the Mecoptera (sensu stricto), which is supported by the male sperm pump that consists of a pistillum and a pumping chamber (Willmann, 1987, 1989; Mickoleit, 2008; Boudinot, 2018). Controversially, a monophyletic Mecoptera is supported as Boreidae + (Nannochoristidae + [Bittacidae + Panorpidae]) inferred from genomic data (Misof *et al.*, 2014). However, recent molecular studies suggest that Siphonaptera is potentially sister to Nannochoristidae, and probably should be treated as an infraorder within Mecoptera (Meusemann *et al.*, 2020; Tihelka *et al.*, 2020).

The species-poor Panorpodidae (short-faced scorpionflies) and the diverse Panorpidae (scorpionflies) are the most derived families of Pistillifera (Willmann, 1987, 1989; Bicha, 2018; Nakamura *et al.*, 2019). In the Panorpidae, two major clades were revealed by recent phylogenetic analyses based exclusively on DNA sequence data (Hu *et al.*, 2015; Miao *et al.*, 2019), but a comprehensive phylogenetic analysis based on morphological characters is still lacking. Historically, the Panorpidae consists

Correspondence: Bao-Zhen Hua, College of Plant Protection, Northwest A&F University, Yangling, Shaanxi 712100, China. E-mail: huabzh@nwafu.edu.cn

of three subfamilies: Panorpinae, Choristinae and Nannochoristinae (Esben-Petersen, 1921). The latter two were raised to familial status along with Panorpodidae by Byers (1965), resulting in a sole retention of the nominotypical subfamily thereafter. The Panorpidae currently consists of approximately 500 extant species in eight genera: the Holarctic *Panorpa* Linnaeus (ca. 260 spp.), the Indonesian-endemic *Leptopanorpa* MacLachlan (14 spp.), the Oriental *Neopanorpa* van der Weele (ca. 170 spp.) and five Chinese endemic genera: *Cerapanorpa* Gao, Ma & Hua (21 spp.), *Dicerapanorpa* Zhong & Hua (20 spp.), *Furcatopanorpa* Ma & Hua (1 sp.), *Megapanorpa* Wang & Hua (5 spp.) and *Sinopanorpa* Cai & Hua (3 spp.). The Panorpidae are widely dispersed in the subtropical and temperate zones of Eurasia and North America (Penny & Byers, 1979; Wang & Hua, 2017, 2018, 2019a,b; Bicha, 2018; Wang *et al.*, 2019; Hu & Hua, 2020), with a number of species penetrating into the equatorial zones, *e.g.*, the Indian Western Ghats, the Mainland Southeast Asia, the Sunda Islands and the Mexican Plateau (Rust & Byers, 1976; Chau & Byers, 1978; Penny & Byers, 1979; Wang & Hua, 2020).

In contrast, the fossil records of Panorpidae are considerably rare. The monotypic genus †*Baltipanorpa* Krzemiński & Soszyńska-Maj from the Eocene Baltic amber is characterized by the greatly elongated notal and postnotal organs on male T3 and T4 (terga III and IV), respectively (Krzemiński & Soszyńska-Maj, 2012). Seven extinct species are assigned to *Panorpa*: two from the Eocene Baltic amber (Carpenter, 1954), three from the Oligocene German Rott shales (Statz, 1936; Willmann, 1976) and two from the Eocene North American Florissant shales (Scudder, 1890; Cockerell, 1907). When excluding the Jurassic †*Muchoria* Sukatsheva and †*Jurassipanorpa* Ding *et al.*, and the Cretaceous †*Solusipanorpa* Lin from this family (Willmann, 1987; Ding *et al.*, 2014; Soszyńska-Maj *et al.*, 2020), the oldest known fossil species of Panorpidae was reported from the early Eocene (ca. 52.9 mya) of MacAbee, Canada (Archibald *et al.*, 2013).

In general, *Leptopanorpa* and *Neopanorpa* can be differentiated from other panorpid genera by the vein 1A ending proximal to the origin of Rs (ORs) in the forewings (Esben-Petersen, 1921; Cheng, 1957b; Rust & Byers, 1976; Chau & Byers, 1978; Wang & Hua, 2019a). However, a few species of *Neopanorpa* bear a long 1A exceeding ORs (Rust & Byers, 1976), and *Panorpa bashanicola* Hua, Tao & Hua bears a short 1A ending proximal to ORs (Hua *et al.*, 2018), suggesting that more characters should be consulted in the generic assignment for species. Willmann (1989) noted that some *Panorpa* species are in a sister group-relationship to *Leptopanorpa* + *Neopanorpa*, indicating a possible paraphyly of *Panorpa*. Subsequently, the paraphyly of *Panorpa* was supported by both morphological (Ma *et al.*, 2012) and molecular analyses (Misof *et al.*, 2000; Whiting, 2002; Hu *et al.*, 2015; Miao *et al.*, 2019). Similarly, *Neopanorpa* was also considered paraphyletic with *Leptopanorpa* by morphological and molecular studies (Ma *et al.*, 2012; Miao *et al.*, 2019; Wang & Hua, 2020).

The informal category 'species group' is frequently adopted for local faunas of *Panorpa* and *Neopanorpa*. In *Panorpa*, Esben-Petersen (1921) proposed nine groups for the Eurasian fauna, four for the Japanese-East Asian fauna, and three for the North American fauna (excluding the Mexican species). Carpenter (1931) suggested three groups for the North American fauna, and Byers (1993, 1996) added three additional groups into this fauna. Issiki (1933) proposed nine species groups for the fauna of Japan and adjacent countries. Willmann (1977) recognized three groups for the European fauna. In *Neopanorpa*, two species groups were put forward for the southern Indian fauna (Rust & Byers, 1976), and four groups for the Southeast Asian fauna (Chau & Byers, 1978). However, due to the lack of a comprehensive study at the global scale, these species group categories are not consistent in diagnoses, and a large number of species remain unsorted to date.

According to recent molecular studies (Hu *et al.*, 2015; Miao *et al.*, 2019), the Panorpidae can be categorized into two major clades: one consisting of *Leptopanorpa* and *Neopanorpa*, and the other comprising the other extant genera. A great divergence between these two clades is also supported by the morphology of the egg chorion (Ma *et al.*, 2009), the chromosome number (Miao *et al.*, 2019) and the morphology and biology of the larvae (Jiang *et al.*, 2019b). Therefore, taxonomic revisions at the generic levels are desperately needed to provide a clear diagnosis for each clade of Panorpidae, and resolve the paraphyly of *Panorpa* and *Neopanorpa*.

The aims of this study were: (1) to investigate the phylogeny of Panorpidae and test the monophyly of each clade based on morphological characters, and (2) to discuss the evolutionary and biogeographical implications in Panorpidae with regard to the phylogenetic analyses.

Material and methods

Repositories

Specimens examined in this study are deposited in or loaned from the following institutions:

CFYC Fung Ying Cheng's Collection (currently in NWAU)

DALU Dali University, Dali, China

ECAU Entomological Collection, China Agricultural University, Beijing, China

EDKU Entomological Division (formerly Snow Entomological Museum), Biodiversity Institute, University of Kansas, Lawrence, U.S.A.

GTGU Museum of Zoology, University of Göttingen, Göttingen, Germany

KYSU Entomological Laboratory, Kyushu University, Fukuoka, Japan

ISWU Insect Collection of Southwest University, Chongqing, China

MYNU Mianyang Normal University, Mianyang, China

NAKU Nankai University, Tianjin, China

NMCZ Department of Entomology, National Museum, Prague, Czech

NWAU Entomological Museum, Northwest A&F University, Yangling, China

OMGM Omogo Mountain Museum, Kumakogen, Japan
SCAU South China Agricultural University, Guangzhou, China
SHNU Insect Collection of Shanghai Normal University, Shanghai, China
SYSU Sun Yat-sen University, Guangzhou, China
TJNH Tianjin Natural History Museum, Tianjin, China
UGIC University of Guelph Insect Collection, Guelph, Canada

Morphological study and taxonomy

Specimens were observed and dissected under a Motic K-401 L CMO Stereo Microscope (Motic, Hongkong, China). Genitalia were macerated in boiling 10% NaOH solution for 3–5 min and rinsed with tap water. Photographs were taken with a Nikon D7000 digital camera (Nikon, Tokyo, Japan) in conjunction with a Nikkor AF-S Micro 105 mm f/2.8 lens, or a Canon MP-E 65 mm f/2.8 1-5X macro lens (Canon, Tokyo, Japan) with a handmade mount adapter. Line-art was drawn based on micro-images with Adobe Illustrator CC. All figures were assembled with Adobe Photoshop CC.

The assignment of 18 species groups (16 in *Panorpa* and two in *Neopanorpa*) follows Esben-Petersen (1921), Carpenter (1931, 1938), Rust & Byers (1976), Chau & Byers (1978), Willmann (1977) and Byers (1993, 1996). Fourteen groups (eight in *Panorpa* and six in *Neopanorpa*) are newly proposed based on morphological affinities (see key to subfamilies, genera and species groups). The *P. davidi* group sensu Esben-Petersen (1921), the *N. denticulata* group sensu Rust & Byers (1976) and the *N. muelleri* group sensu Chau & Byers (1978) are revised to include or exclude certain species. The *P. leucoptera* group sensu Issiki (1933) is renamed as the *P. nikkoensis* group since *P. nikkoensis* Miyaké was synonymized with *P. leucoptera* Uhler due to a misidentification, but recently revalidated by Miyamoto & Nakamura (2008). The *P. rufescens* group sensu Byers (1993) is renamed as the *P. confusa* group because *P. rufescens* Rambur was synonymized with *P. confusa* Westwood by Somma (2011). Names and related information for each examined taxon are listed in the Supporting Information Table S1.

Terminology of the external morphology follows Mickoleit (1975, 1976, 1978) and Willmann (1977, 1987, 1989). The following abbreviations are used: A1, the first abdominal segment (and so forth for other segments); T1, the first tergum (and so forth for other terga); S1, the first sternum (and so forth for other sterna). Dagger symbol '†' indicates fossil taxa.

Phylogenetic analysis

A total of 155 species of Panorpidae were selected as ingroup taxa, accounting for approximately 31% of the extant species, including all the 32 recognized species groups (24 in *Panorpa* and eight in *Neopanorpa*), and all the eight extant genera. The type species of all the genera are included in the analysis except *Neopanorpa*, the type species of which, *N. angustipennis* (Westwood), is unavailable at present. The fossil species of *Panorpa* and †*Baltipanorpa* are not analysed owing to their barely known genital morphology. According to Willmann (1983, 1989), Choristidae is sister to Panorpidae + Panorpodidae among the extant families. Therefore, two species of Choristidae, *Chorista australis* Klug and *Taeniochorista nigrita* Riek and three species of Panorpodidae, *Panorpodes kuandianensis* Zhong, Zhang & Hua, *Po. paradoxa* MacLachlan, and *Brachypanorpa carolinensis* (Banks), were selected as outgroup taxa. Information for the taxa is listed in the Supporting Information Table S1.

Morphological characters were observed by the first author, or inferred from works cited. The characters were partially adopted or modified from those used by Ma *et al.* (2012), Soszyńska-Maj *et al.* (2020), and Wang & Hua (2020). Unavailable character states were coded as '?'; and inapplicable as '-'. A total of 182 morphological characters (162 binary and 20 multistate) of adults were encoded as follows:

Head (Fig. 1)

1 Ocellar bristles: present (0) (Fig. 1A–D); absent (1) (Fig. 1I).
2 Compound eyes: narrower than middle of rostrum (0) (Fig. 1B); enlarged, as wide as or wider than middle of rostrum (1) (Fig. 1J, K).
3 Length of rostrum: short, approximately as long as wide (0) (Fig. 1C); slightly elongated, at most twice as long as wide (1) (Fig. 1B); greatly elongated and slender, at least three times as long as wide (2) (Fig. 1E).
4 Shape of rostrum: stout, evenly tapering towards apex (0) (Fig. 1I); slender, with approximately parallel lateral margins (1) (Fig. 1K).
5 Sclerotized ring basal to maxillary palpomere III: absent (0) (Fig. 1Q–T); present (1) (Fig. 1U, V).

Thorax (Fig. 2)

6 Stout setae on posterior margin of pronotum: present (0) (Fig. 2A, B); absent (1) (Fig. 2C).
7 Stout setae on mesonotum: present (0) (Fig. 2A, B); absent (1) (Fig. 2C).
8 Comb-like preapical teeth on inner margin of pretarsal claws: present (0) (Fig. 2F, H–J); absent or greatly reduced (1) (Fig. 2G).
9 Second preapical tooth of pretarsal claws, if present: approximately the same size as others (0) (Fig. 2H); greatly enlarged (1) (Fig. 2I).
10 Three preapical teeth of pretarsal claws, if present: arising from a more or less straight line (0) (Fig. 2H); arising from a bulge (1) (Fig. 2J).

Wings (Fig. 3)

11 Ratio of forewing widths at ending of M_4 to 1A: < 2 (0) (Fig. 3A); ≥ 2 (1) (Fig. 3D).
12 Costal margin of forewing: arched (0) (Fig. 3A); straight (1) (Fig. 3B).

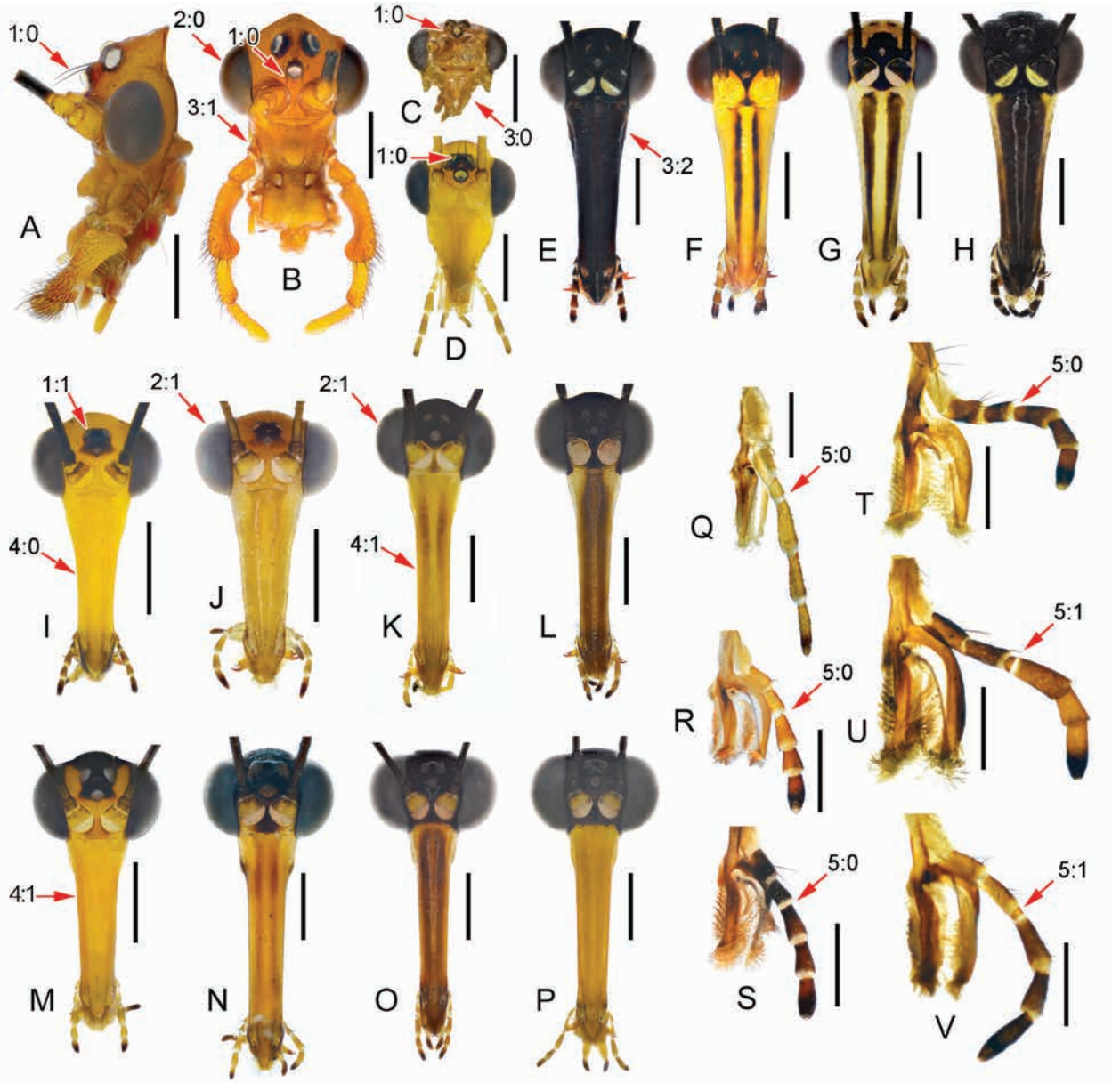

Fig. 1. Head. (A,B) Head, frontal view except (A) in lateral view; (Q–V) right maxilla, posterior view. (A,B) *T. nigrita* Riek; (C) *B. carolinensis* (Banks); (D) *Po. paradoxa* MacLachlan; (E,S) *P. bicornuta* MacLachlan; (F,R) *P. leucoptera* Uhler; (G) *D.* sp.; (H) *M. grandis* Wang & Hua; (I) *P. jinhuaensis* Wang, Gao & Hua; (J) *P. kunmingensis* Fu & Hua; (K) *N. chillcotti* Byers; (L) *N. muelleri* (van der Weele); (M) *N. harmandi* (Navás); (N,V) *N. brisi* (Navás); (O) *L. cingulata* (Enderlein); (P) *L. linyejiei* Wang & Hua; (Q) *Po. kuandianensis* Zhong, Zhang & Hua; (T) *P. pryeri* MacLachlan; (U) *P. amurensis* MacLachlan. Character numbers and states are indicated by arrows (and so forth for other figures). Scale bars: 1.0 mm in (A–P), and 0.5 mm in (Q–V). [Colour figure can be viewed at wileyonlinelibrary.com].

13 Costal veinlets: two or more (0) (Fig. 3A); one (1) (Fig. 3B); absent (2) (Fig. 3C).
14 Branches of M in forewing: five (0) (Fig. 3A); four (1) (Fig. 3B, C).
15 Base of M_4 in forewing: straight (0) (Fig. 3B); curved (1) (Fig. 3C).
16 Base of M_{3+4} in forewing: as long as or longer than m-cu (0) (Fig. 3B, C); shorter than m-cu (1) (Fig. 3D).
17 1A ending in forewing: beyond or near origin of Rs (ORs) (0) (Fig. 3A); proximal to ORs (1) (Fig. 3D).
18 Ratio of distances between ending of 1A and 2A to CuP in hindwing: ≥ 1 (0) (Fig. 3A); < 1 (1) (Fig. 3D).
19 Number of anal cross-veins a between 1A and 2A in forewing: more than three (0) (Fig. 3A); two or three (1) (Fig. 3C); one (2) (Fig. 3B).

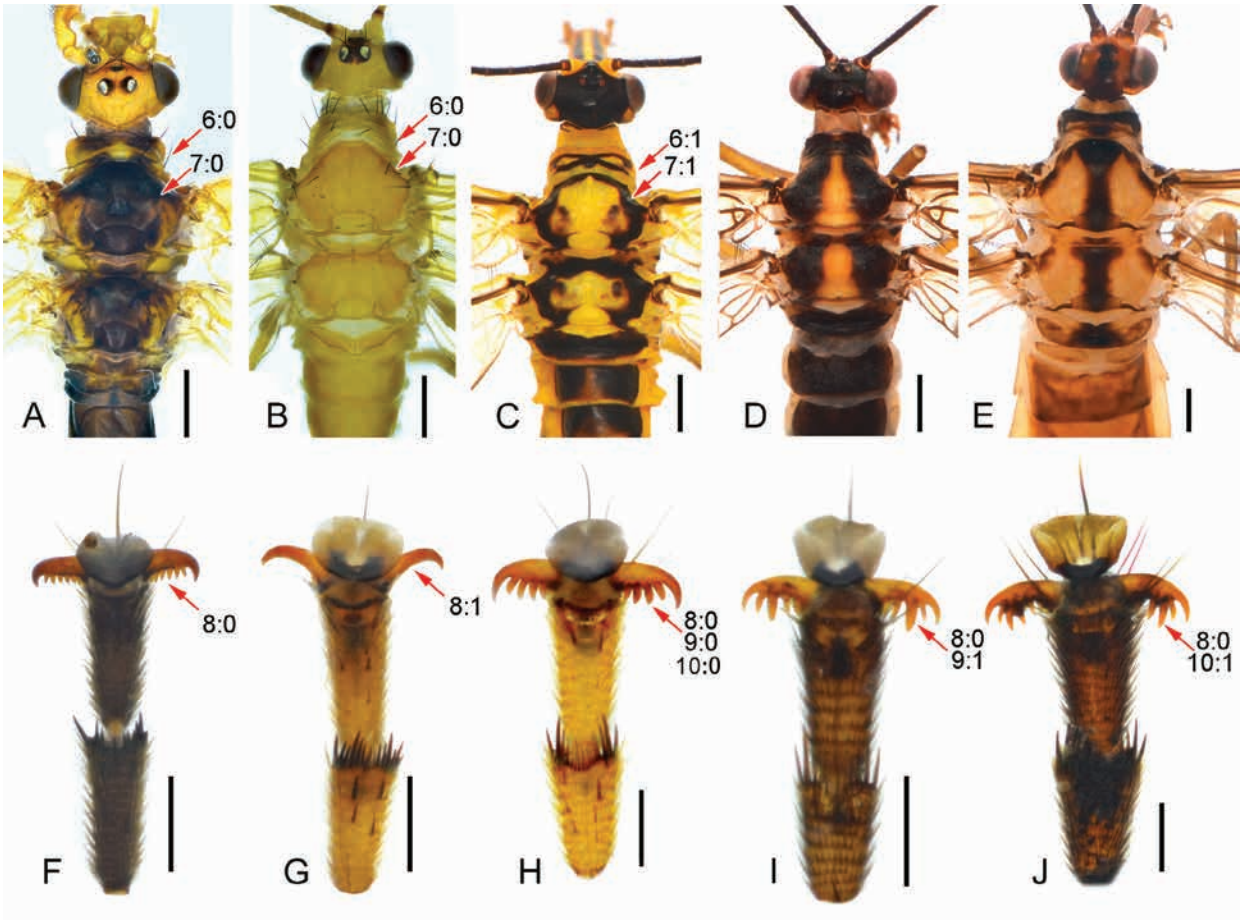

Fig. 2. Head and thorax. (A–E) Head and thorax, dorsal view; (F–J) distal two tarsomeres and pretarsus of hind legs, ventral view. (A,F) *T. nigrita* Riek; (B) *Po. paradoxa* MacLachlan; (C) *P. leucoptera* Uhler; (D) *P. sonani* Issiki; (E) *N. k-maculata* Cheng; (G) *Po. kuandianensis* Zhong, Zhang & Hua; (H) *S. tincta* (Navás); (I) *L. cingulata* (Enderlein); (J) *N. nielseni* Byers. Scale bars: 0.5 mm in (A–E), and 0.2 mm in (F–J). [Colour figure can be viewed at wileyonlinelibrary.com].

20 cu-a in hindwing: absent (0) (Fig. 3H); present (1) (Fig. 3I).
21 Anterior ending of a in hindwing: proximal to fork of CuP+1A (0) (Fig. 3H); distal to the latter (1) (Fig. 3I).
22 Base of 1A in hindwing: straight (0) (Fig. 3H); curved at a (1) (Fig. 3I).
23 Stout setae on base of 2A in forewing: present (0) (Fig. 3F, G); absent (1) (Fig. 3C).

Male abdomen (Figs. 4, 5, 9)

24 Sternal organ on S2: absent (0) (Fig. 5C); present (1) (Fig. 5E).
25 Poststernal spines on S2–S5: absent (0) (Fig. 4N); present (1) (Fig. 4O).
26 Notal organ on T3: absent or undeveloped (0) (Fig. 4A, B); present and well-developed (1) (Fig. 4C).
27 Shape of notal organ, if present and well-developed: short, overlapping postnotal organ on T4 (0) (Fig. 4C); slightly elongated, not extending to middle of T4 (1) (Fig. 4M); long and clavate, exceeding middle but not exceeding hind border of T4 (2) (Figs. 4G, 5B, D); long and clavate, exceeding hind border of T4 (3) (Figs. 4D, 5A, C).
28 Base of notal organ: simple (0) (Fig. 5I); expanded, wider than twice the width of apex (1) (Fig. 5L).
29 Small tooth-like projection under notal organ: absent (0) (Fig. 5K); present (1) (Fig. 5M).
30 Paired small teeth aside notal organ on posterior border of T3: absent (0) (Fig. 5I); present (1) (Fig. 5N).
31 Postnotal organ on T4: absent (0) (Fig. 4A); present (1) (Fig. 4B, C, L, M).
32 Shape of postnotal organ, if present: acute (0) (Fig. 4L, M); blunt or rounded (1) (Fig. 5J, K); depressed with a series of long setae (2) (Fig. 4D).
33 Position of postnotal organ on T4: at anterior portion (0) (Fig. 4L, M); at approximately middle (1) (Fig. 5J, K); at hind border (2) (Fig. 4D, G).
34 Direction of postnotal organ: curved dorso-cephalad (0) (Fig. 4L, M); dorsad (1) (Fig. 5J, K).
35 Membranous region on anterior portion of T4: absent (0) (Fig. 5I); present (1) (Fig. 5L).

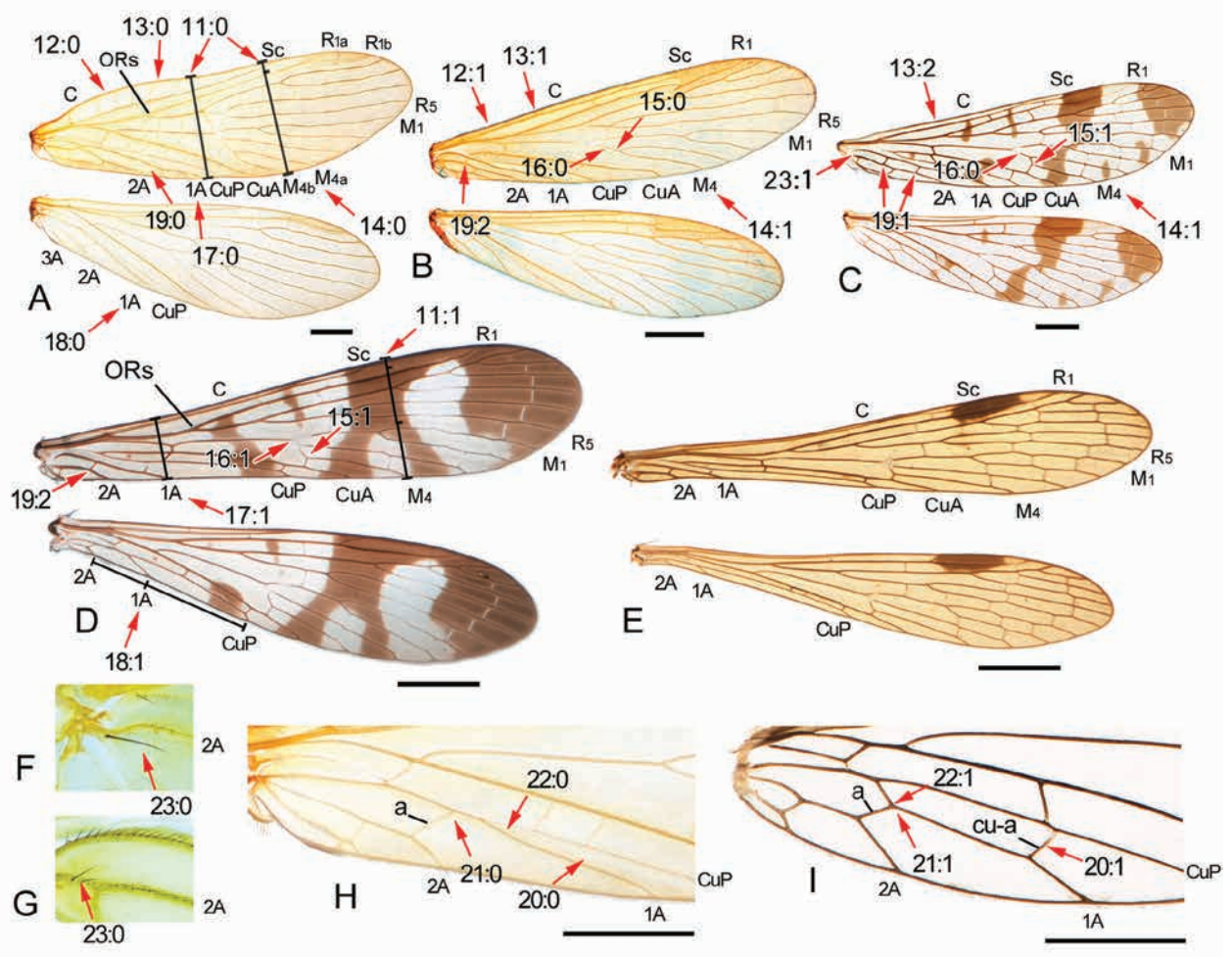

Fig. 3. Wings. (A,F,H) *T. nigrita* Riek; (B,G) *Po. paradoxa* MacLachlan; (C) *P. communis* Linnaeus; (D) *N. pulchra* Carpenter; (E) *L. cingulata* (Enderlein); (I) *D. diceras* (MacLachlan). Scale bars: 2.0 mm. [Colour figure can be viewed at wileyonlinelibrary.com].

36 Pleural membrane of A6, or at least a fusion seam: present (0) (Fig. 4A, B); absent, with tergum and sternum entirely fused (1) (Fig. 4C).
37 Length of A6: approximate to A5 (0) (Fig. 4A, B); longer than but no more than twice of A5 (1) (Fig. 4C, D); a least twice as long as A5 (2) (Fig. 4G).
38 Apical half of A6: cylindrical, or evenly tapering towards truncate apex (0) (Fig. 4F); abruptly tapering towards conical apex (1) (Fig. 4H).
39 Anal horns on dorsal apex of A6: absent (0) (Fig. 4F); one (1) (Fig. 4I, J); two (2) (Fig. 4K).
40 Paired subapical claws on T6: absent (0) (Fig. 5C); present (1) (Fig. 5E, G, H).
41 Apex of A6: truncated (0) (Fig. 4F); beveled (1) (Fig. 4G).
42 Distal emargination of A6: absent (0) (Fig. 4F); present as a pair of triangular lobes laterally (1) (Fig. 4N).
43 Dense setae on middle of T6: absent (0) (Fig. 4F); present (1) (Fig. 4H).
44 Dorsal apex of T6: unmodified (0) (Fig. 4E); raised dorsad with dense long setae (1) (Fig. 4G).
45 Lateral notch of A6: absent (0) (Fig. 5E); present (1) (Fig. 5F).
46 Length of A7: shorter than or equal to A5 (0) (Fig. 4A); longer than but no more than three times of A5 (1) (Figs. 4E, F, 5C); at least three times as long as A5 (2) (Figs. 4G, 5B, E, F).
47 Shape of A7: unmodified or slightly constricted basally (0) (Fig. 4A); constricted basally and evenly thicker towards apex (1) (Fig. 4D, F); constricted basally and greatly thicker towards apex, forming a basal stalk (2) (Fig. 4H).
48 Pleural membrane of A7, or at least a fusion seam: present (0) (Fig. 4A, B); absent, with tergum and sternum entirely fused (1) (Fig. 4C).
49 Middle portion of A7: unmodified (0) (Fig. 4I); buckling medially, break-like (1) (Fig. 4J).
50 Dorsal apex of A7: simple (0) (Fig. 4E); raised dorsad (1) (Fig. 4N).

51 Apex of T7: simple (0) (Fig. 4A); emarginate (1) (Fig. 4C).
52 Latero-dorsal apex of T7: simple (0) (Fig. 5G); greatly projected (1) (Fig. 5O).
53 Latero-ventral apex of S7: simple (0) (Fig. 4E); protruded horn-like (1) (Fig. 4C).
54 Length of A8: shorter than or equal to A5 (0) (Fig. 4A, B); elongated but no more than twice of A5 (1) (Fig. 4C); elongated, much longer than twice of A5 (2) (Figs. 4E, 5B, E, F).
55 Shape of A8: not constricted basally (0) (Fig. 4B); constricted basally (1) (Fig. 4F).
56 Shape of S10: flat (0) (Fig. 9B); greatly protruding ventrad (1) (Fig. 9F).

Male genitalia (Figs. 4–11).

The male genitalia comprise two large clasping appendages (gonopods), which are fused basally and surround the aedeagal complex, and are cupped by the single sclerite of the ninth abdominal segment. The ninth segment has dorsal and ventral portions, namely, the epandrium (Fig. 9A–G) and hypandrium ('hyp', Fig. 6B), respectively. On the ventral surface of the epandrium are sometimes a pair of epandrial lobes ('epl', Fig. 9B). The hypandrium is usually produced as a pair of hypovalves distally, and on the inner base of each hypovalve there is sometimes a hypandrial process ('hpr', Fig. 9J, K). The gonopods are two-segmented, comprising the proximal gonocoxites ('gcx', Fig. 6B, 7A, 8A) and distal gonostyli ('gs',

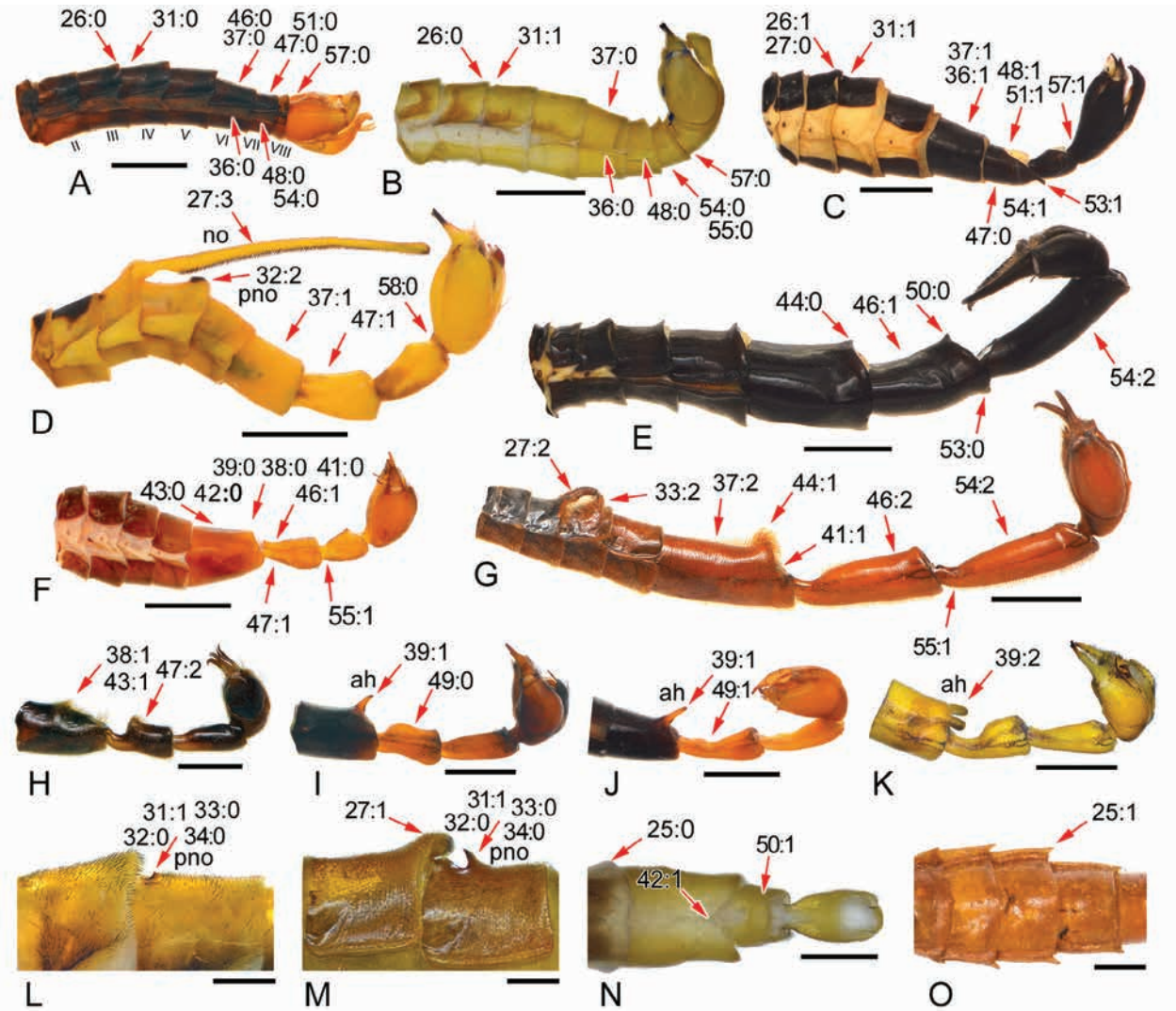

Fig. 4. Abdomen. (A–G) Abdomen, lateral view; (H–K) A6–A11, lateral view; (L,M) T3 and T4, lateral view; (N) A6–A8, dorsal view; (O) A2–A5, dorsal view. (A) *T. nigrita* Riek; (B,L) *Po. kuandianensis* Zhong, Zhang & Hua; (C) *P. bicornuta* MacLachlan; (D) *P. takenouchii* Miyaké; (E) *P. ishiharai* Miyamoto; (F) *P. communis* Linnaeus; (G) *P. stigmalis* Navás; (H) *S. nangongshana* Cai & Hua; (I) *M. gaokaii* Wang & Hua; (J) *C. obtusa* (Cheng); (K) *D. magna* (Chou); (M) *P. amurensis* MacLachlan; (N) *P. kunmingensis* Fu & Hua; (O) *P. lugubris* Swederus. ah, anal horn; no, notal organ; pno, postnotal organ. Scale bars: 2.0 mm in (A–K), and 1.0 mm in (L–O). [Colour figure can be viewed at wileyonlinelibrary.com].

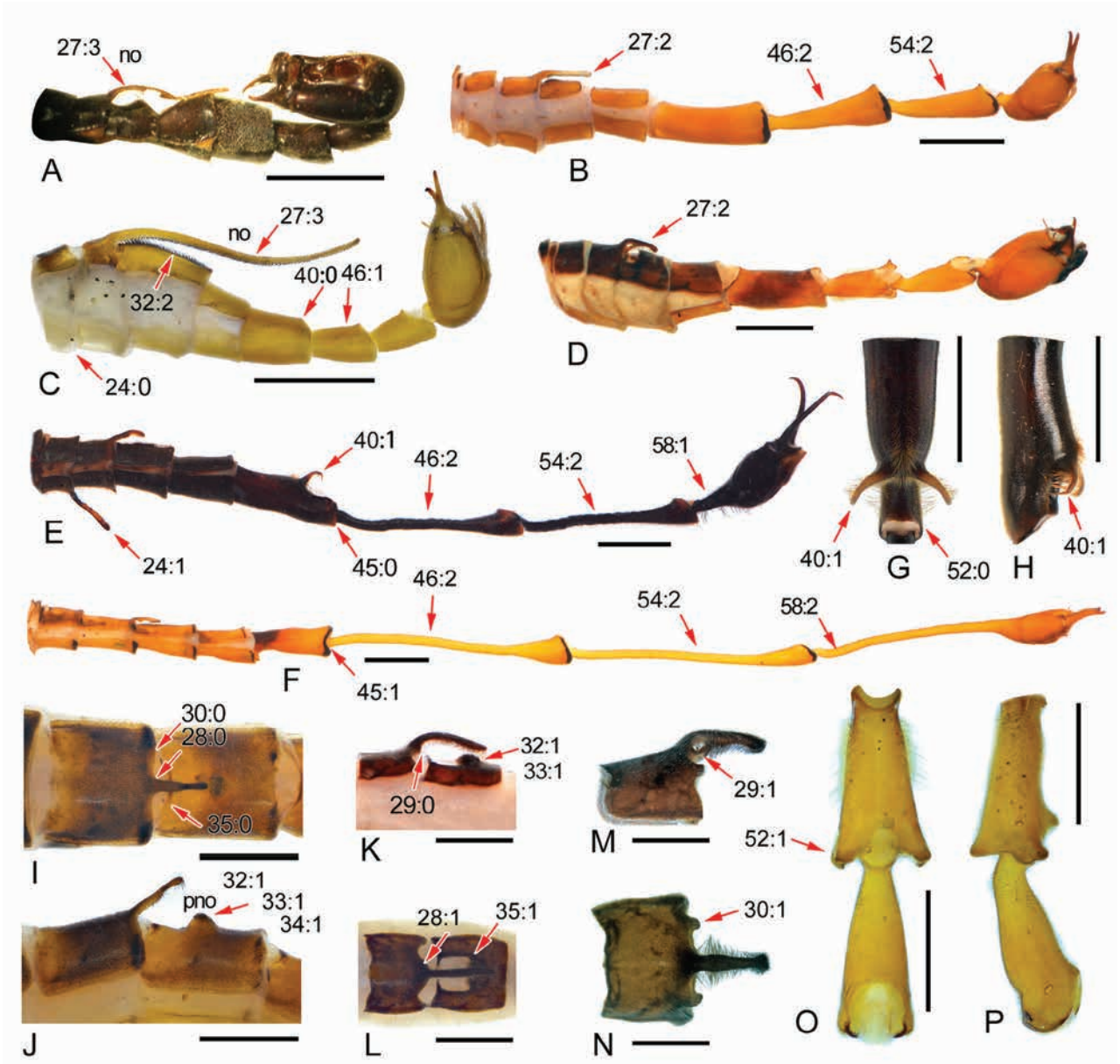

Fig. 5. Abdomen. (A–F) Abdomen, lateral view; (G,O) A7 and A8, dorsal view; (H,P) A7 and A8, lateral view; (I,L) T3 and T4, dorsal view; (J,K) T3 and T4, lateral view; (M,N) T3, lateral and dorsal views, respectively. (A) *N. appendiculata* (Westwood); (B) *N. chillcotti* Byers; (C) *N. choui* Cheng; (D), (M–P) *N. brisi* (Navás); (E,G,H) *N. furcata* (Hardwicke); (F) *L. linyejiei* Wang & Hua; (I,J) *L. cingulata* (Enderlein); (K,L) *N. mutabilis* Cheng. no, notal organ; pno, postnotal organ. Scale bars: 2.0 mm in (A–H), (O,P), 1.0 mm in (I–L), and 0.5 mm in (M,N). [Colour figure can be viewed at wileyonlinelibrary.com].

Fig. 6B, 7A, 8A). The gonostylus is elongated, and bears a median tooth ('mt', Fig. 7H) and a basal process ('bp', Fig. 7H) on the inner margin. The aedeagal complex (Figs. 10, 11) is composed of a pair of ventral valves ('vv', Fig. 10A–C), a pair of dorsal valves ('dv', Fig. 10B, C), a pair of dorsal processes ('dpr', Fig. 10B, C), a pair of lateral processes ('lpr', Fig. 10A–C), dorso-basally, a piston of sperm pump ('pst', Fig. 10B, C), and ventrally, a pair of parameres ('pm', Fig. 10A). The paramere bears a basal stalk ('stp', Fig. 10A–C) and frequently a modified distal part (furcated, curled or bearing bristles). Although the term 'paramere' is widely adopted in Mecoptera, it must be noted that this structure is not homologous with those in other holometabolous orders. For example, the 'parameres' in Coleoptera are best supported as homologs with the gonopods in Mecoptera (Boudinot, 2018).

57 Base of A9: thick (0) (Fig. 4A, B); constricted (1) (Fig. 4C).

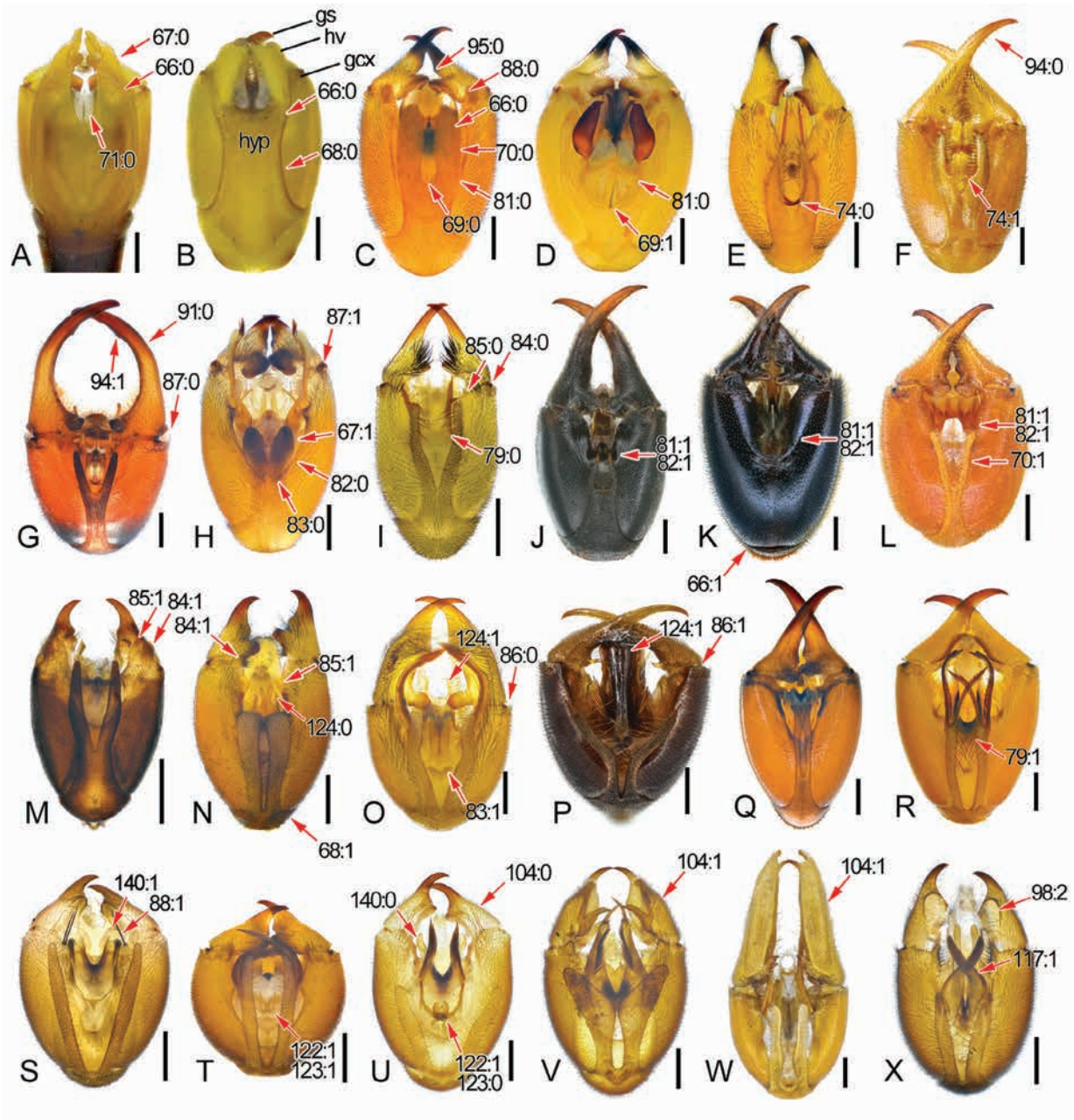

Fig. 6. Male genitalia, ventral view. (A) *T. nigrita* Riek; (B) *Po. kuandianensis* Zhong, Zhang & Hua; (C) *P. leucoptera* Uhler; (D) *P. takenouchii* Miyaké; (E) *P. jinhuaensis* Wang, Gao & Hua; (F) *P. amurensis* MacLachlan; (G) *P. nipponensis* Navás; (H) *P. striata* Issiki; (I) *P. guttata* Navás; (J) *P. lugubris* Swederus; (K) *P. truncata* Byers; (L) *P. bimacula* Byers; (M) *P. sibirica* Esben-Petersen; (N) *P. germanica* Linnaeus; (O) *P. cladocerca* Navás; (P) *P. emeishana* Hua, Sun & Li; (Q) *P. stigmalis* Navás; (R) *P. aurea* Cheng; (S) *P. helena* Byers; (T) *P. alpina* Rambur; (U) *P. latipennis* Hine; (V) *P. galerita* Byers; (W) *P. mirabilis* Carpenter; (X) *P. curva* Carpenter. gcx, gonocoxite; gs, gonostylus; hv, hypovalve; hyp, hypandrium. Scale bars: 0.5 mm. [Colour figure can be viewed at wileyonlinelibrary.com].

58 Stalk of A9: short, inconspicuous (0) (Fig. 4D); elongated, but not longer than gonocoxites (1) (Fig. 5E); greatly elongated, longer than gonocoxites (2) (Figs. 5F, 8M).

59 Apex of epandrium: not emarginate or indistinctly emarginate (0) (Fig. 9A); emarginate, forming a pair of stout lateral processes (1); deeply emarginate, forming a pair of slender finger-like processes (2) (Fig. 9G).

60 Terminal projection of epandrium: absent (0) (Fig. 9A); present (1) (Fig. 9B).

61 Latero-subapical projection of epandrium: simple (0) (Fig. 9A); projected (1) (Fig. 9D).

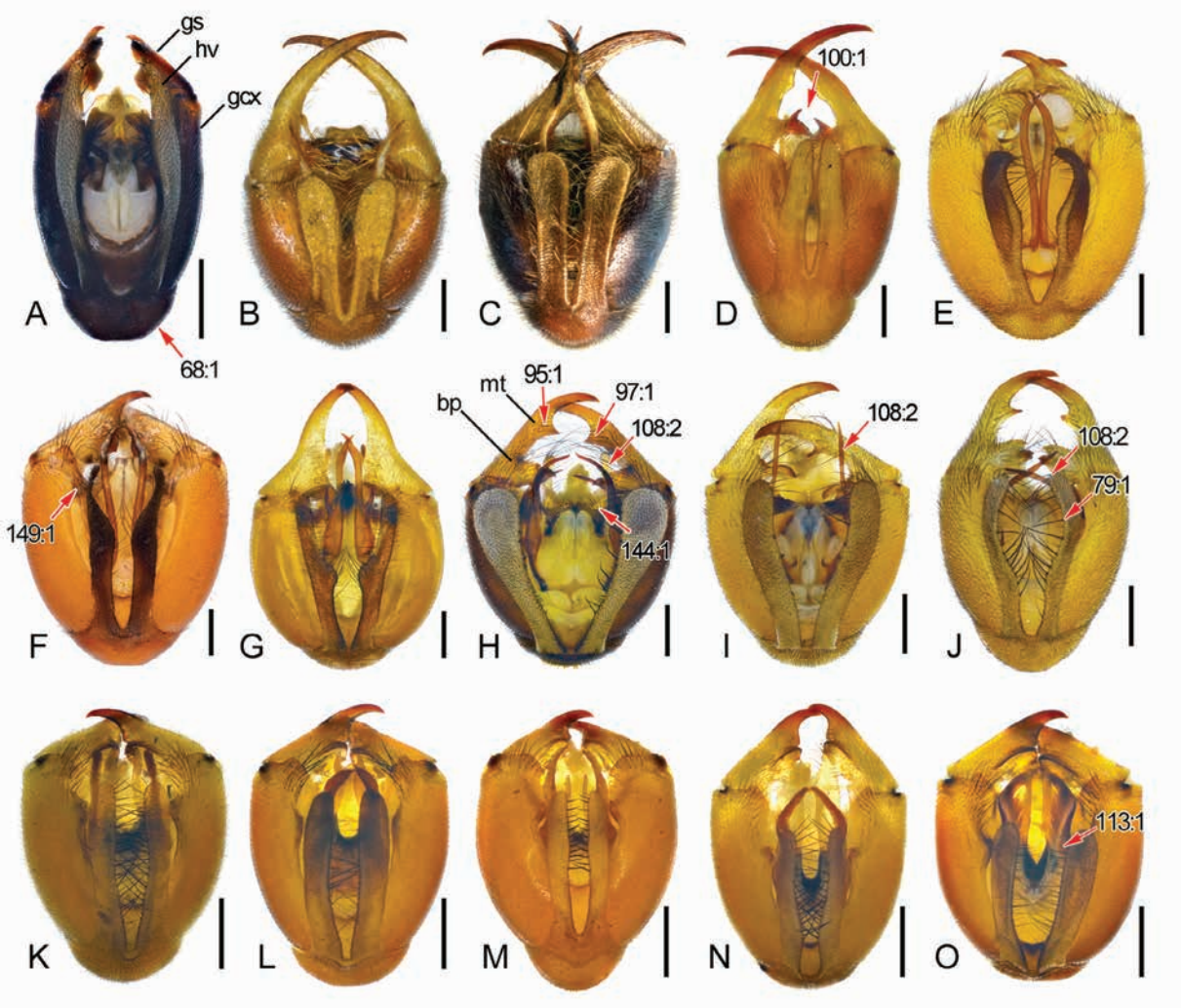

Fig. 7. Male genitalia, ventral view. (A) *F. longihypovalva* (Hua & Cai); (B) *S. digitiformis* Huang & Hua; (C) *S. nangongshana* Cai & Hua; (D) *S. tincta* (Navás); (E) *M. absens* Wang & Hua; (F) *M. grandis* Wang & Hua; (G) *M. wanghongjiani* Wang & Hua; (H) *D. diceras* (MacLachlan); (I) *D. kimminsi* (Carpenter); (J) *D. magna* (Chou); (K) *C. dubia* (Chou & Wang); (L) *C. liupanshana* Gao, Ma & Hua; (M) *C. brevicornis* (Hua & Li); (N) *C. nanwutaina* (Chou); (O) *C. obtusa* (Cheng). bp, basal process; gcx, gonocoxite; gs, gonostylus; hv, hypovalve; mt, median tooth. Scale bars: 0.5 mm. [Colour figure can be viewed at wileyonlinelibrary.com].

62 Lateral margins of epandrium: almost parallel (0) (Fig. 9A); subtriangular, tapering towards acute apex (1) (Fig. 9E).
63 Epandrial lobe: absent (0) (Fig. 9F); present (1) (Fig. 9B).
64 Size of epandrial lobe, if present: small and narrow, invisible from above (0) (Fig. 9B); greatly enlarged and projected laterad, visible from above (1) (Fig. 9C).
65 Apex of epandrial lobe in lateral aspect: rounded or truncated (0) (Fig. 9C); acute (1) (Fig. 9B).
66 Hypandrium: well-developed (0) (Fig. 6A, B, C); entirely reduced (1) (Fig. 6K).
67 Length of hypandrium: exceeding middle of gonocoxites (0) (Fig. 6A); greatly shortened, not exceeding middle of gonocoxites (1) (Fig. 6H).
68 Basal stalk of hypandrium: long and distinct (0) (Fig. 6B); greatly shortened (1) (Fig. 6N).
69 Distal setae of hypandrial basal stalk: absent (0) (Fig. 6C); present (1) (Fig. 6D).
70 Shape of hypovalve: broad, stripe-like (0) (Fig. 6C); extremely narrow, thread-like (1) (Fig. 6L).
71 Hypovalves with inner margin: widely separated, untouched (0) (Fig. 8B, C); overlapped (1) (Fig. 8E).
72 Hypovalve with outer margin: unfolded (0) (Fig. 9I); slightly folded dorsad (1) (Fig. 9J); greatly folded dorsad then mesad, forming a boat-shaped structure (2) (Fig. 9L).
73 Subapical process on inner side of hypovalve: absent (0) (Fig. 8C); present (1) (Fig. 8A, B).

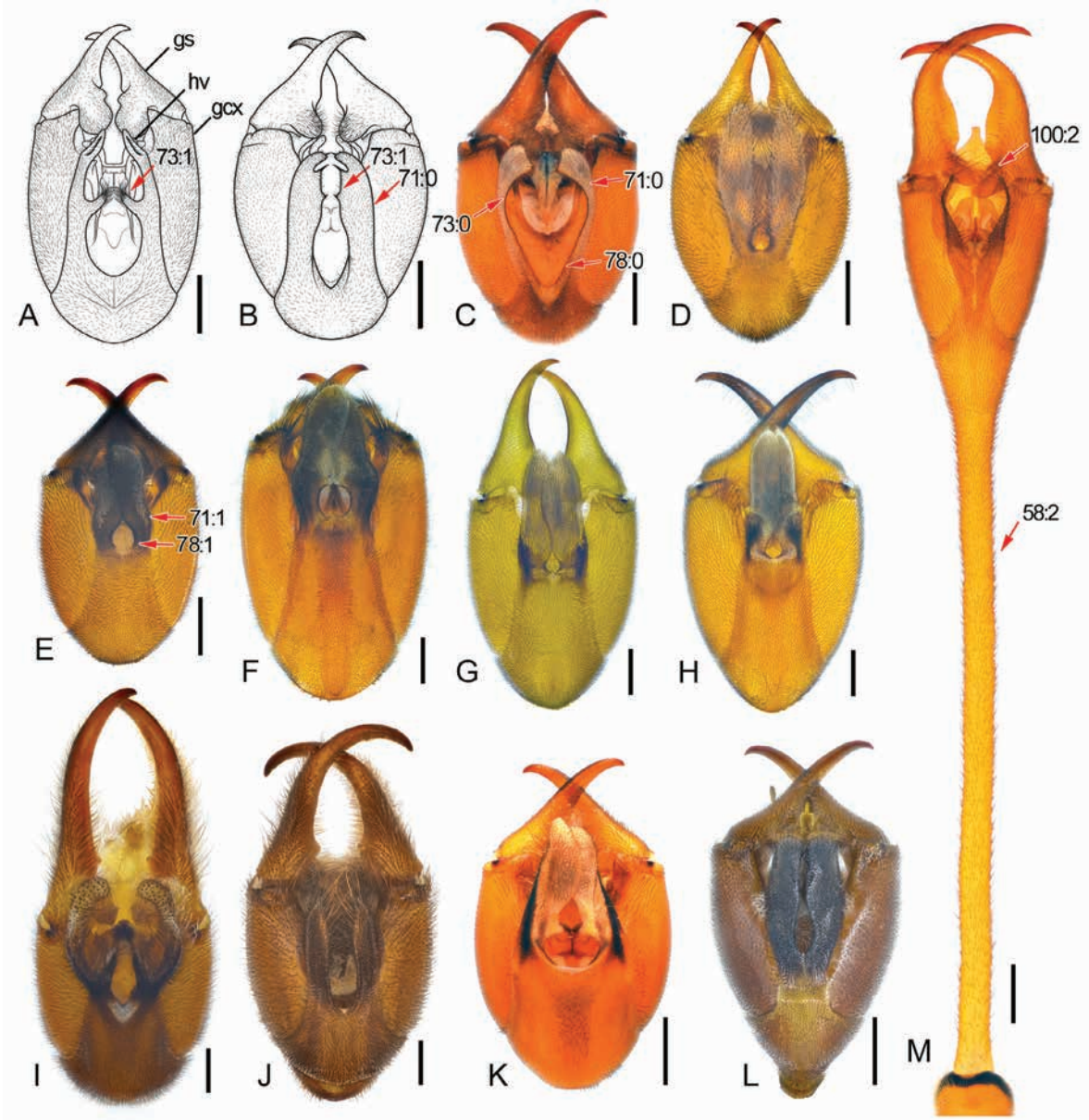

Fig. 8. Male genitalia, ventral view. (A) *N. appendiculata* (Westwood); (B) *N. denticulata* Rust & Byers; (C) *N. chillcotti* Byers; (D) *N. choui* Cheng; (E) *N. muelleri* (van der Weele); (F) *N. brisi* (Navás); (G) *N. cavaleriei* (Navás); (H) *N. nielseni* Byers; (I) *N. k-maculata* Cheng; (J) *N. magna* Issiki; (K) *N. gradana* Cheng; (L) *L. cingulata* (Enderlein); (M) *L. linyejiei* Wang & Hua. gcx, gonocoxite; gs, gonostylus; hv, hypovalve. Scale bars: 0.5 mm. [Colour figure can be viewed at wileyonlinelibrary.com].

74 Subtriangular projection directed caudo-mesad at basal third of inner margin of hypovalve: absent (0) (Fig. 6E); present (1) (Fig. 6F).
75 Rectangular projection directed cephalo-mesad on subbasal portion of inner margin of hypovalve: absent (0) (Fig. 9I); present (1) (Fig. 9M).
76 Rectangular subbasal projection on outer margin of hypovalve: absent (0) (Fig. 9J); present (1) (Fig. 9L).
77 Basal constriction of hypovalves: no (0) (Fig. 9I); yes (1) (Fig. 9K).
78 Basal subcircular window formed by hypovalves: absent (0) (Fig. 8C); present (1) (Fig. 8E).
79 Setae along inner margin of hypovalve: uniformly sized with those in other regions (0) (Fig. 6I); longer and stouter than those in other regions (1) (Fig. 6R).
80 Hypandrial processes at inner base of hypovalves: absent (0) (Fig. 9H, I); present (1) (Fig. 9J, K).
81 Shape of gonocoxital concavity in ventral aspect: broad, exceeding middle of gonocoxites (0) (Fig. 6C, D);

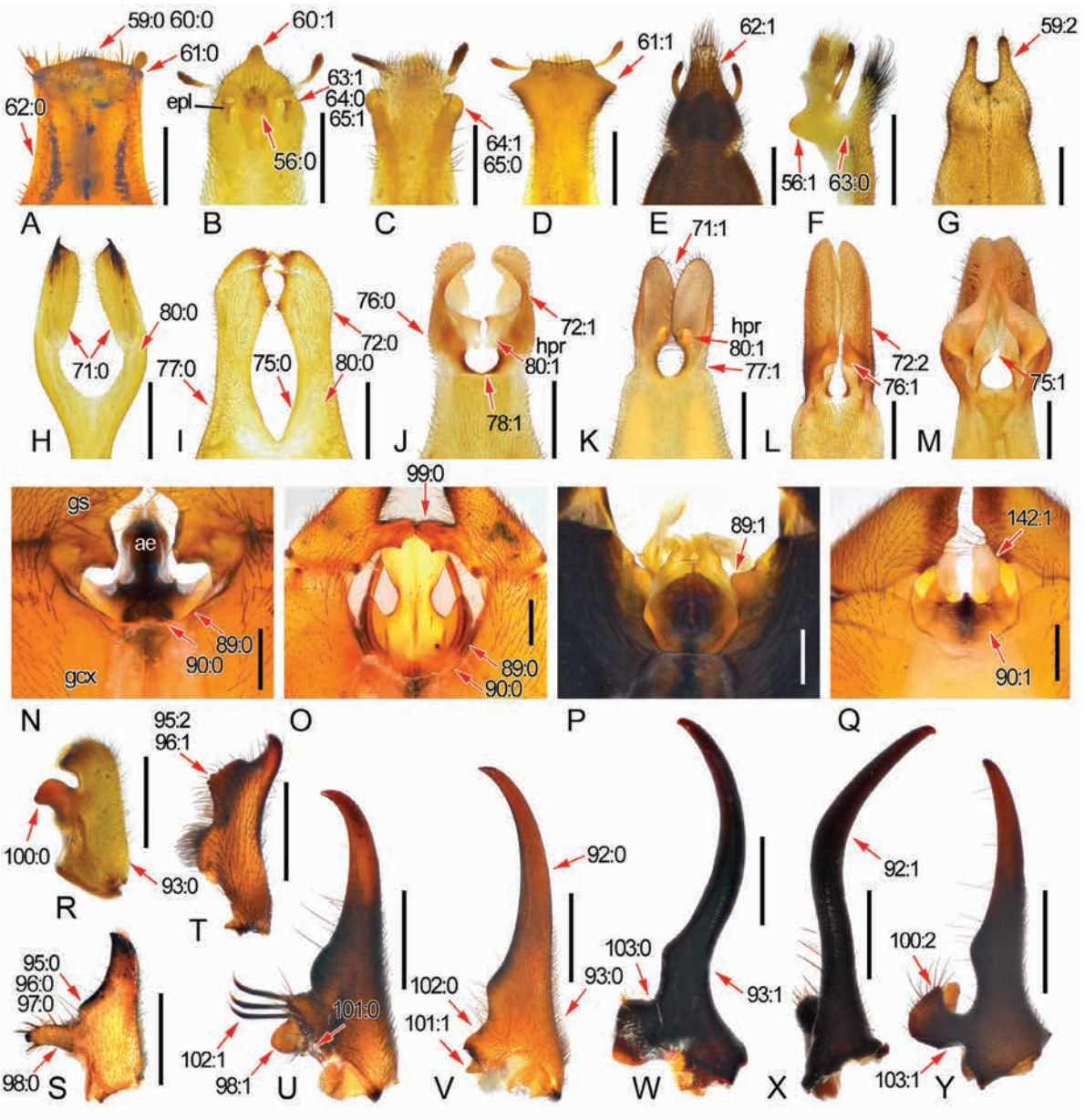

Fig. 9. Male genitalia. (A–G) Apical portion of epandrium (T9), dorsal view except (B) in ventral view, and (F) in lateral view; (H–M) apical portion of hypandrium (S9), dorsal view; (N–Q) details of genital bulb, dorsal view; (R–Y) gonostylus, ventral view except (X) in lateral view. (A,R) *T. nigrita* Riek; (B) *L. cingulata* (Enderlein); (C) *N. ovata* Cheng; (D) *N. pendula* Qian & Zhou; (E) *P. lugubris* Swederus; (F) *P. sibirica* Esben-Petersen; (G) *P. emeishana* Hua, Sun & Li; (H) *Po. paradoxa* MacLachlan; (I) *N. denticulata* Rust & Byers; (J) *N. tienpingshana* Chou & Wang; (K) *N. longiprocessa* Hua & Chou; (L), (N,V) *N. nielseni* Byers; (M) *N. brisi* (Navás); (O) *P. pryeri* MacLachlan; (P) *P. amurensis* MacLachlan; (Q) *P. communis* Linnaeus; (S) *Po. kuandianensis* Zhong, Zhang & Hua; (T) *F. longihypovalva* (Hua & Cai); (U) *N. muelleri* (van der Weele); (W,X) *P. baohwashana* Cheng; (Y) *L. majapahita* Wang & Hua. ae, aedeagus; epl, epandrial lobe; gcs, gonocoxites; gs, gonostylus. Scale bars: 0.5 mm. [Colour figure can be viewed at wileyonlinelibrary.com].

relatively narrow and shallow, not exceeding middle of gonocoxites (1) (Fig. 6J–L).

82 Bottom of gonocoxital concavity: rounded (0) (Fig. 6H); subtrapezoidal (1) (Fig. 6J–L).

83 M-shaped process at joint of gonocoxites ventrally: absent (0) (Fig. 6H); present (1) (Fig. 6O).

84 Terminal plate of gonocoxite: absent (0) (Fig. 6I); present (1) (Fig. 6M, N).

85 Medial spine of gonocoxite: absent (0) (Fig. 6I); present (1) (Fig. 6M, N).

86 Shape of gonocoxites: nearly parallel (0) (Fig. 6O); widely divergent towards apexes (1) (Fig. 6P).

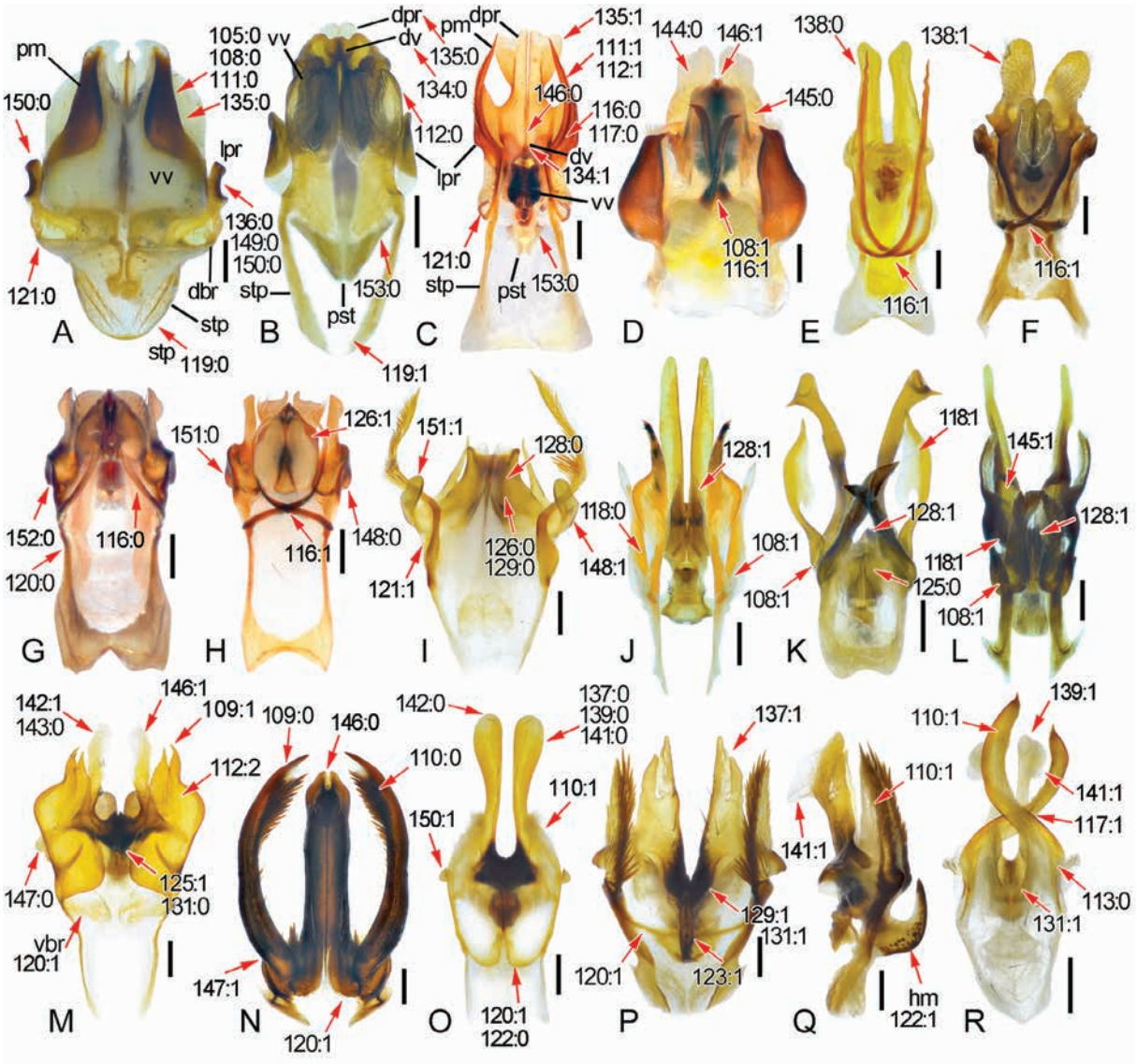

Fig. 10. Male aedeagal complex. Ventral view except (Q) in lateral view. (A) *T. nigrita* Riek, 1973; (B) *Po. paradoxa* MacLachlan; (C) *P. pryeri* MacLachlan; (D) *P. takenouchii* Miyaké; (E) *P. jinhuaensis* Wang, Gao & Hua; (F) *P. amurensis* MacLachlan; (G) *P. japonica* Thunberg; (H) *P. nipponensis* Navás; (I) *P. gressitti* Byers; (J) *P. azteca* Byers; (K) *P. involuta* Byers; (L) *P. lugubris* Swederus; (M) *P. communis* Linnaeus; (N) *P. semifasciata* Cheng; (O) *P. dashahensis* Zhou & Zhou; (P,Q) *P. cornigera* MacLachlan; (R) *P. sexspinosa* Cheng. dbr, dorsal bridge of paramere; dpr, dorsal process; hm, hamulus; lpr, lateral process; pm, paramere; stp, stalk of paramere; vbr, ventral bridge of paramere; vv, ventral valve. Scale bars: 0.2 mm. [Colour figure can be viewed at wileyonlinelibrary.com].

87 Ventral apex of gonocoxites: nearly truncated (0) (Fig. 6G); strongly beveled (1) (Fig. 6H).
88 Long setae on inner apex of gonocoxite: absent (0) (Fig. 6C); present (1) (Fig. 6S).
89 Triangular process on dorsal apex of gonocoxite: absent (0) (Fig. 9N, O); present (1) (Fig. 9P).
90 A pair of fused lobes on dorsal apex of gonocoxites: absent (0) (Fig. 9N, O); present (1) (Fig. 9Q).
91 Length of gonostylus: shorter than or approximately as long as gonocoxites (0) (Fig. 6G); much longer than the latter (1) (Issiki, 1933, fig. 10H).
92 Distal half of gonostylus: uncurved or slightly curved (0) (Fig. 9V); greatly curved dorsad (1) (Fig. 9X).
93 Basal portion of gonostylus: straight or indistinctly curved (0) (Fig. 9V); greatly curved mesad (1) (Fig. 9W).
94 Series of small protuberances on inner margin of gonostylus: absent (0) (Fig. 6F); present (1) (Fig. 6G).
95 Shape of median tooth of gonostylus: indistinct (0) (Fig. 9S); stout and acute, but not wider than diameter of gonostylus (1) (Fig. 7H); greatly enlarged, wider than diameter of gonostylus (2) (Fig. 9T).

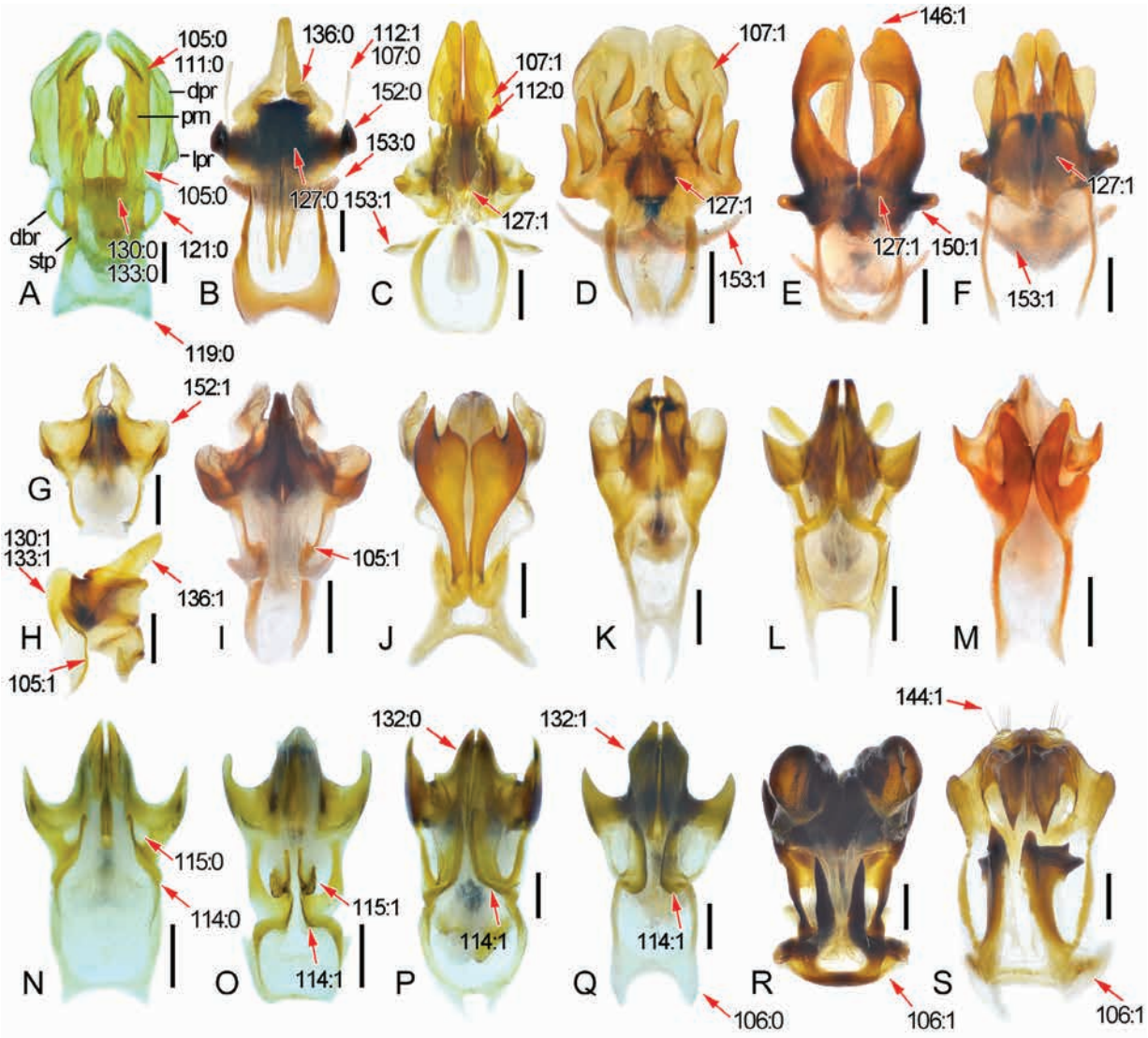

Fig. 11. Male aedeagal complex, ventral view except (H) in lateral view. (A) *N. denticulata* Rust & Byers; (B) *N. chillcotti* Byers; (C) *L. cingulata* (Enderlein); (D) *L. linyejiei* Wang & Hua; (E) *L. nematogaster* (MacLachlan); (F) *L. majapahita* Wang & Hua; (G,H) *N. muelleri* (van der Weele); (I) *N. fuscicauda* Chau & Byers; (J) *N. choui* Cheng; (K) *N. moganshanensis* Zhou & Wu; (L) *N. longiprocessa* Hua & Chou; (M) *N. nigritis* Carpenter; (N) *N. claripennis* Carpenter; (O) *N. tienmushana* Cheng; (P) *N. fangxianga* Zhou & Zhou; (Q) *N. nielseni* Byers; (R) *N. k-maculata* Cheng; (S) *N. magna* Issiki. dbr, dorsal bridge of paramere; dpr, dorsal process; lpr, lateral process; pm, paramere; stp, stalk of paramere. Scale bars: 0.2 mm. [Colour figure can be viewed at wileyonlinelibrary.com].

96 Inner margin of median tooth of gonostylus: smooth (0) (Fig. 9S); serrate (1) (Fig. 9T).

97 Position of median tooth: close to subbasal process (0) (Fig. 9S); beyond middle of gonostylus and far away from basal process (1) (Fig. 7H).

98 Ventral concaved region of basal process: absent or indistinct (0) (Fig. 9S); present but small, not longer than basal diameter of gonostylus (1) (Fig. 9U); present, longer than basal diameter of gonostylus (2) (Fig. 6X).

99 Apex of basal process: rounded or evenly tapering (0) (Fig. 9O); abruptly tapering towards acute tooth (1) (Cheng, 1957b, figs. 86, 88).

100 Furcation of basal process: simple (0) (Fig. 9R); bifurcated at middle (1) (Fig. 7D); bifurcated at base (2) (Fig. 8M).

101 Small tooth-like basal process of basal process: absent (0) (Fig. 9U); present (1) (Fig. 9V).

102 Thick setae on basal process: absent (0) (Fig. 9V); present (1) (Fig. 9U).

103 Base of basal process: simple (0) (Fig. 9W); distinctly constricted (1) (Fig. 9Y).

104 Accessory lobe on ventral surface of gonostylus: absent (0) (Fig. 6U); present (1) (Fig. 6V, W).

105 Parameres: well-developed (0) (Figs. 10A, 11A); greatly reduced, with only a basal stalk present (1) (Fig. 11H, I).

106 Basal stalk of paramere: simple (0) (Fig. 11Q); greatly curved dorsad (1) (Fig. 11R, S).
107 Relation of paramere with dorsal process: separated (0) (Fig. 11B); fused (1) (Fig. 11C, D).
108 Paramere furcated basally: unbranched (0) (Fig. 10A); bifurcated (1) (Fig. 10J, K, L); trifurcated (2) (Fig. 7H, I, J).
109 Furcation of paramere beyond middle: unbranched (0) (Fig. 10N); bifurcated (1) (Fig. 10M).
110 Inner margin of paramere: sclerotized (0) (Fig. 10N); membranous (1) (Fig. 10O, Q, R).
111 Surface of paramere: glabrous or with a few microtrichia (0) (Fig. 10A); with numerous microtrichia or long spines (1) (Fig. 10C).
112 Shape of paramere: short, blunt (0) (Fig. 10B); greatly elongated, stick-like or filiform (1) (Fig. 10C); greatly expanded, blade-like or foliate (2) (Fig. 10M).
113 Paramere enlarged near basal stalk: not enlarged (0) (Fig. 10R); enlarged, approximately two times as wide as distal portion (1) (Fig. 7O); enlarged, wider than three times of distal portion (2) (Li *et al.*, 2007, fig. 2B).
114 Parameres curved subbasally: uncurved or only slightly curved (0) (Fig. 11N); greatly curved mesad and then caudad (1) (Fig. 11O, P, Q).
115 Direction of apex of paramere: caudad (0) (Fig. 11N); greatly bent ventrad (1) (Fig. 11O).
116 Parameres crossed subbasally, proximal to ventral aedeagal valves: not crossed (0) (Fig. 10C, G); crossed (1) (Fig. 10D, E, F, H).
117 Parameres crossed subdistally, distal to ventral aedeagal valves: not crossed (0) (Fig. 10C); crossed (1) (Fig. 10R).
118 Swollen dorsal process of paramere: absent (0) (Fig. 10J); present (1) (Fig. 10K, L).
119 Lamella connecting two basal stalks of parameres: present (0) (Fig. 10A); absent (1) (Fig. 10B).
120 Ventral bridge of paramere connected to ventral aedeagal valves: absent (0) (Fig. 10G); present (1) (Fig. 10M, N, O, P).
121 Dorsal bridge of paramere: present (0) (Figs. 10C, 11A); greatly vestigial or absent (1) (Fig. 10I).
122 Aedeagal hamulus (sensu Byers, 1993): absent (0) (Fig. 10O); present (1) (Figs. 6T, 10Q).
123 Shape of hamulus, if present: simple, rounded apically (0) (Fig. 10); bifurcated, slender and acute apically (1) (Figs. 6T, 10P).
124 Apex of aedeagus: concealed in gonocoxital concavity, approximate to or slightly exceeding apex of gonocoxites (0) (Fig. 6N); greatly exceeding apex of gonocoxites (1) (Fig. 6O, P).
125 A melanized triangular area basal to aedeagus: absent (0) (Fig. 10K); present (1) (Fig. 10M).
126 Swelling of ventral valves: simple (0) (Fig. 10I); greatly swollen (1) (Fig. 10H).
127 Reduction of ventral valves: not reduced (0) (Fig. 11B); greatly reduced (1) (Fig. 11C, D, E, F).
128 Ventral valves projected ventrad: not projected (0) (Fig. 10I); projected, beak-like (1) (Fig. 10J, K, L).
129 Ventral valves: closely adjoining (0) (Fig. 10I); widely divergent (1) (Fig. 10P).
130 Ventral valves flattening: not flattened (0) (Fig. 11A); greatly flatten and blade-like (1) (Fig. 11H).
131 Sharp oblique ridge of ventral valve: absent (0) (Fig. 10M); present (1) (Fig. 10P, R).
132 Wide shoulder-like lateral projection of ventral valve: absent (0) (Fig. 11P); present (1) (Fig. 11Q).
133 Broadly ventral protrusion of ventral valves: not protruded (0) (Fig. 11A); protruded (1) (Fig. 11H).
134 Dorsal valves: simple (0) (Fig. 10B); surrounded by lateral wall formed by ventral valves and dorsal processes (1) (Fig. 10C).
135 Elongation of dorsal process: not elongated (0) (Fig. 10B); greatly elongated (1) (Fig. 10C).
136 Direction of dorsal process: caudad (0) (Fig. 11B); caudo-dorsad (1) (Fig. 11H).
137 Furcation of dorsal process: simple (0) (Fig. 10O); bifurcated subapically (1) (Fig. 10P).
138 Shape of dorsal process: simple (0) (Fig. 10E); flattened and setose (1) (Fig. 10F).
139 Ventral curving of apical third of dorsal process: not curved (0) (Fig. 10O); greatly curved (1) (Fig. 10R).
140 Dorso-basal bending of apical third of dorsal process: not bending (0) (Fig. 6U); greatly bending (1) (Fig. 6S).
141 A swollen membranous process on dorso-subapical portion of dorsal process: absent (0) (Fig. 10O); present (1) (Fig. 10Q, R).
142 Apex of dorsal process: sclerotized (0) (Fig. 10O); membranous and slightly enlarged (1) (Fig. 10M).
143 Basal portion of dorsal process: simple (0) (Fig. 10M); greatly constricted, neck-like (1) (Wang & Hua, 2017, fig. 5).
144 Stout setae on dorsal process: absent (0) (Fig. 10D); present (1) (Figs. 7H, 11S).
145 A concaved basal region of dorsal process: absent (0) (Fig. 10D); present (1) (Fig. 10L).
146 Two dorsal processes: closely adjoining at base (0) (Fig. 10C); separated basally (1) (Fig. 10D).
147 Reduction of lateral process of aedeagus: not reduced (0) (Fig. 10M); reduced, indistinct (1) (Fig. 10N).
148 Elongation of lateral process of aedeagus: not elongated (0) (Fig. 10H); greatly elongated (1) (Fig. 10I).
149 Fusion of lateral process with gonocoxites: not fused (0) (Fig. 10A); fused (1) (Fig. 7F).
150 Direction of lateral process: caudad (0) (Fig. 10A); laterad (1) (Fig. 11E).
151 Curving of lateral process: simple (0) (Fig. 10H); greatly curved inward and enclosing paramere (1) (Fig. 10I).
152 Shape of lateral process: small and narrow (0) (Fig. 11B); greatly expanded and broad (1) (Fig. 11G).
153 Lateral process of piston of sperm pump: short, not reaching lateral processes (0) (Fig. 11B); greatly elongated, approximately reaching or exceeding lateral processes (1) (Fig. 11C).

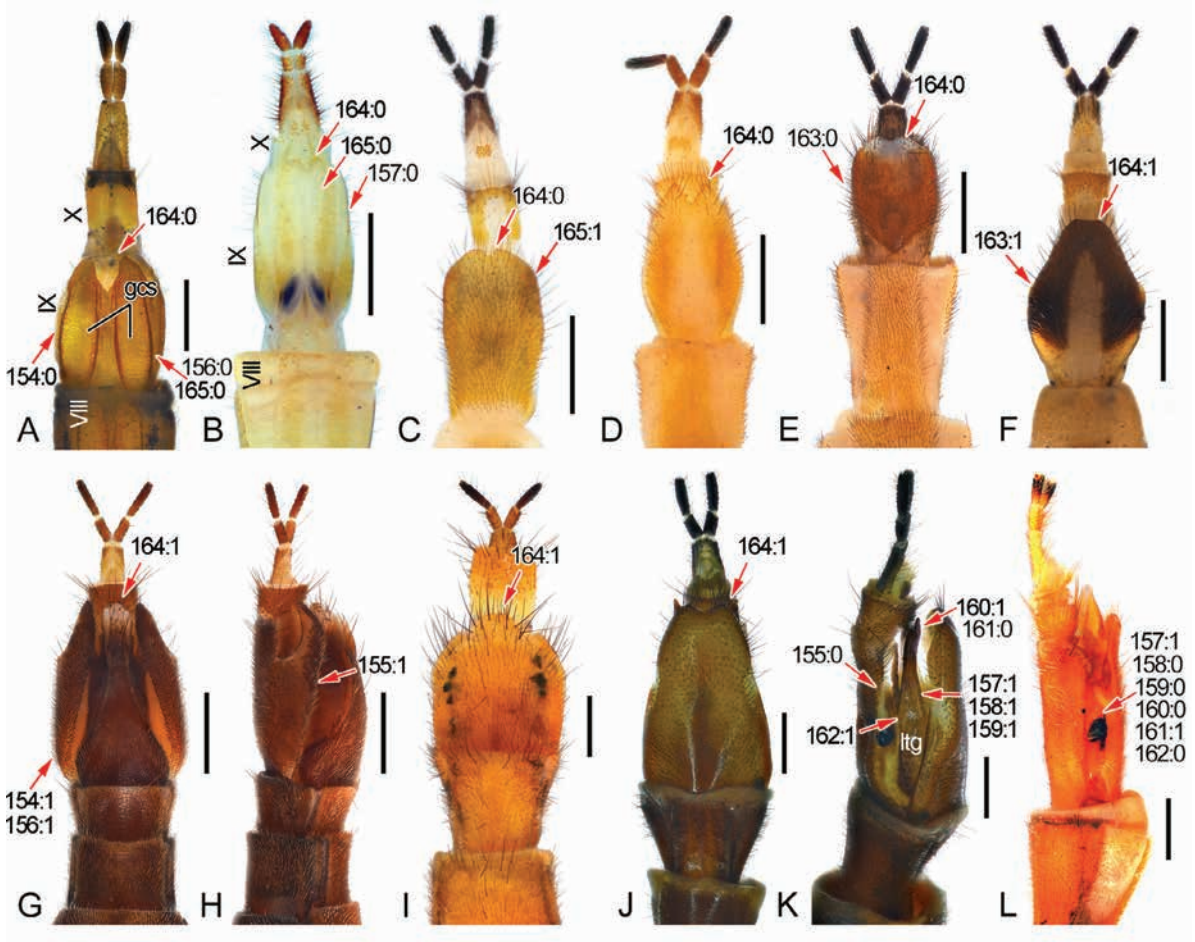

Fig. 12. Female terminal abdomen, ventral view except (H), (K,L) in lateral view. (A) *T. nigrita* Riek; (B) *Po. kuandianensis* Zhong, Zhang & Hua; (C) *L. cingulata* (Enderlein); (D) *N. chillcotti* Byers; (E) *N. muelleri* (van der Weele); (F) *P. gressitti* Byers; (G,H) *P. emeishana* Hua, Sun & Li; (I) *D. magna* (Chou); (J,K) *M. jiangorum* Wang & Hua; (L) *S. tincta* (Navás). gcs, gonocoxosternite; ltg, laterotergite. Scale bars: 0.5 mm. [Colour figure can be viewed at wileyonlinelibrary.com].

Female abdomen (Fig. 12)

154 Length of A9: approximate to A8 (0) (Fig. 12A); longer than A8 (1) (Fig. 12G).
155 Lateral margins of T9: unmodified (0) (Fig. 12K); curled ventrad, enclosing subgenital plate (1) (Fig. 12H).
156 Width of T9: approximately as wide as T8 (0) (Fig. 12A); distinctly wider than T8 (1) (Fig. 12G).

Female genitalia (Figs. 12, 13).

The female genitalia comprise a subgenital plate (Fig. 12) and a medigynium (Fig. 13, = genital plate, or internal skeleton). The subgenital plate is modified from a pair of gonocoxosternites VIII (Mickoleit, 1975), and presented by two separate plates in Choristidae (Fig. 12A) and Panorpodidae (Fig. 12B), and fused as one in Panorpidae (Fig. 12C–L). On the lateral sides of the subgenital plate, there is sometimes a pair of laterotergites ('ltg', Fig. 12K). Inside the genital chamber enclosed by T9 and the subgenital plate, there is a sclerotized plate, medigynium (Fig. 13), which comprises a main plate ('mp', Fig. 13E), an axis ('ax', Fig. 13E), and usually a pair of posterior arms ('pa', Fig. 13E). The axis is proximally split into a pair of apodemes ('ap', Fig. 13E).

157 Laterotergites: absent or indistinct (0) (Fig. 12B); present and distinct (1) (Fig. 12K, L).
158 Length of laterotergites, if present: shorter than half of subgenital plate (0) (Fig. 12L); approximately as long as subgenital plate (1) (Fig. 12K).
159 Shape of laterotergites, if present: flat, plate-like (0) (Fig. 12L); stick-like with longitudinal ridges (1) (Fig. 12K).
160 Apex of laterotergites, if present: simple (0) (Fig. 12L); bifurcated (1) (Fig. 12K).
161 Apical portion of laterotergites, if present: simple (0) (Fig. 12K); fused with subgenital plate (1) (Fig. 12L).

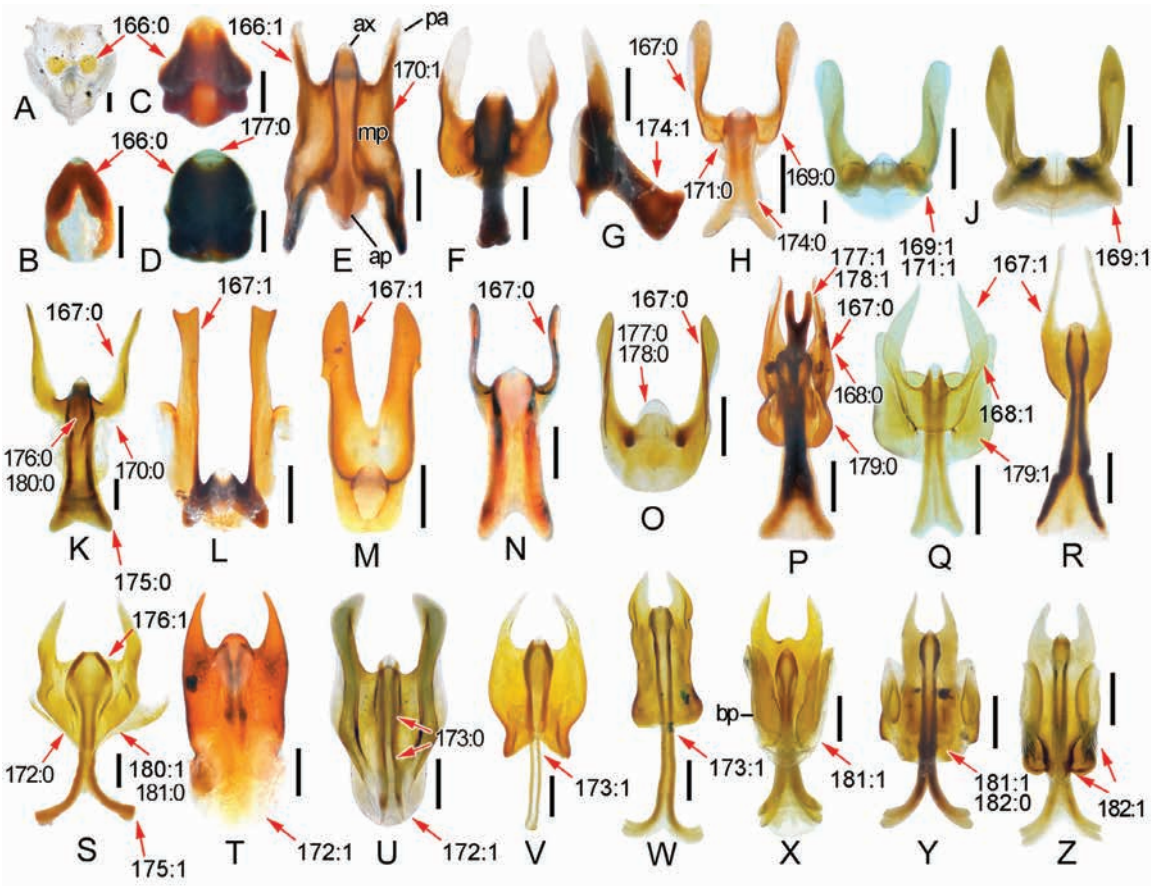

Fig. 13. Female medigynium, ventral view except (G) in lateral view. (A) *T. nigrita* Riek; (B) *B. carolinensis* (Banks); (C) *Po. kuandianensis* Zhong, Zhang & Hua; (D) *Po. paradoxa* MacLachlan; (E) *L. nematogaster* (MacLachlan); (F,G) *L. peterseni* Lieftinck; (H) *N. nigritis* Carpenter; (I) *N. sauteri* (Esben-Petersen); (J) *N. nielseni* Byers; (K) *P. pryeri* MacLachlan; (L) *P. globulifera* Miyamoto; (M) *P. takenouchii* Miyaké; (N) *P. amurensis* MacLachlan; (O) *P. japonica* Thunberg; (P) *F. longihypovalva* (Hua & Cai); (Q) *P. obliquifascia* (Chou & Wang); (R) *P. kunmingensis* Fu & Hua; (S) *P. communis* Linnaeus; (T) *M. grandis* Wang & Hua; (U) *D. magna* (Chou); (V) *P. dashahensis* Zhou & Zhou; (W) *S. tincta* (Navás); (X) *P. debilis* Westwood; (Y) *P. sexspinosa* Cheng; (Z) *C. nanwutaina* (Chou). ap, apodeme of axis; ax, axis; mp, main plate; pa, posterior arm. Scale bars: 0.2 mm. [Colour figure can be viewed at wileyonlinelibrary.com].

162 Inner margin of laterotergites, if present: not fused with medigynium (0) (Fig. 12L); fused with medigynium (1) (Fig. 12K).
163 Lateral margin of subgenital plate: smooth (0) (Fig. 12E); projected laterad at middle (1) (Fig. 12F).
164 Apex of subgenital plate: deeply emarginate in a V-shape (0) (Fig. 12A–E); simple or shallowly emarginate (1) (Fig. 12F).
165 Gonocoxosternites VIII of subgenital plate: divided (0) (Fig. 12A, B); fused (1) (Fig. 12C).
166 Posterior arms of medigynium: absent (0) (Fig. 13A–D); present (1) (Fig. 13E).
167 Shape of posterior arm, if present: twisted (0) (Fig. 13H, K, N, O, P); not twisted (1) (Fig. 13L, M, Q, R).
168 Middle portion of posterior arm, if present: simple (0) (Fig. 13P); projecting laterad (1) (Fig. 13Q).
169 Earlobe-like process basal to posterior arm: absent (0) (Fig. 13H); present (1) (Fig. 13I, J).
170 Main plate of medigynium: poorly developed (0) (Fig. 13K); well-developed (1) (Fig. 13E).
171 Shape of main plate: narrower than or approximately as wide as long (0) (Fig. 13H); much wider than long (1) (Fig. 13I).
172 Anterior margin of main plate: sclerotized (0) (Fig. 13S); less sclerotized or membranous, and thinner than posterior portion (1) (Fig. 13T, U).
173 Thickness of basal portion of axis: as thick as or thicker than distal portion (0) (Fig. 13U); very slender, thinner than distal portion (1) (Fig. 13V, W).
174 Apodemes of axis: not curved (0) (Fig. 13H); greatly curved dorsad (1) (Fig. 13G).
175 Basal apex of apodemes of axis: simple (0) (Fig. 13K); branched (1) (Fig. 13S).
176 Decorated area of axis: almost as wide as or slightly wider than middle of axis (0) (Fig. 13K); greatly enlarged, at least two times as wide as the rest portion (1) (Fig. 13S).

177 Apex of axis: almost concealed in main plate or slightly exceeding main plate, not longer than half the latter (0) (Fig. 13O); prominently exceeding main plate, longer than half length of the latter (1) (Fig. 13P).
178 Furcation of apex of axis: simple (0) (Fig. 13O); bifurcated (1) (Fig. 13P).
179 A broad dorsal plate attached to medigynium: absent (0) (Fig. 13P); present (1) (Fig. 13Q).
180 A ventral plate attached to ventral base of main plate of medigynium: absent (0) (Fig. 13K); present (1) (Fig. 13S).
181 Shape of ventral plate, if present: simple (0) (Fig. 13S); enclosing lateral margin of medigynium (1) (Fig. 13X, Y).
182 Splitting of ventral plate, if present: not divided (0) (Fig. 13Y); subdivided into a pair of dorsal plate and a pair of ventral plate (1) (Fig. 13Z).

The character matrix was built with Mesquite version 3.6.1 (Maddison & Maddison, 2019), and is presented in the Supporting Information File S1 and also deposited in the online repository TreeBASE (http://purl.org/phylo/treebase/phylows/study/TB2:S27458). Under the Maximum Parsimony (MP) criterion, an equal weighting (EW) analysis was conducted with TNT 1.5 (Goloboff & Catalano, 2016) using new technology analysis (Sectorial Search, Ratchet, Drift, Tree Fusing). An implied weighting (IW) analysis was conducted with an optimal concavity constant value (*K*-value) calculated by a TNT script setk.run written by Salvador Arias as used by Santos *et al.* (2015). The *K*-value downweights characters based on their level of homoplasy (Legg *et al.*, 2013), and helps improve the phylogenetic results (Goloboff *et al.*, 2008). The new technology analysis was run under the same parameters as the EW analysis. After the run, the unambiguous characters were mapped on the strict consensus tree with WinClada v1.00.08 (Nixon, 2002). Bootstrap values (BS) (Felsenstein, 1985) and Bremer support values (BR) (Bremer, 1994) were calculated in TNT and marked at the right side of each node for the strict consensus tree. All most parsimonious trees are deposited in the online repository TreeBASE.

A Maximum Likelihood (ML) analysis was performed using IQ-TREE 2 version 2.1.2 (Minh *et al.*, 2020). The model MK + ASC was chosen for the dataset to correct the likelihood conditioned on variable sites. Because ML tree searches may become trapped at local optima, ten independent runs were performed with default settings. Ultrafast Bootstrap values (UFBS) (Hoang *et al.*, 2018) were calculated for each tree with 1000 replicates. The ML trees are presented in the Supporting Information File S2 with UFBS mapped, and are also deposited in the online repository TreeBASE. The highest support values received from one ML tree were mapped at the right side of corresponding nodes of the MP tree.

In the description part, we used the following adverbs for the five ranges of the BS and UFBS: 'weakly' for those smaller than 50; 'moderately' for those larger than or equal to 50 but smaller than 75; 'highly' for those larger than or equal to 75 but smaller than 90; 'very highly' for those larger than or equal to 90 but smaller than 100; and 'maximally' for those of 100.

Biogeographical interpretations

The map was obtained from SimpleMappr (http://www.simplemappr.net) and modified in Adobe Illustrator CC to add the distributional ranges and the putative dispersal routes. Distributional ranges were summarized from the specimens examined, the references cited, and the project 'Panorpidae of the World' on iNaturalist (https://www.inaturalist.org/projects/panorpidae-of-the-world). The Panorpidae originated from Asia (Byers, 1988; Hu *et al.*, 2015; Miao *et al.*, 2019), and the putative dispersal events for each fauna were inferred from corresponding clades in the phylogenetic analyses.

Results

Maximum parsimony (MP) analyses

The equal weighting (EW) analysis generated five most parsimonious trees. These trees are basically consistent in topology, especially the two major clades of Panorpidae, but are slightly inconsistent with respect to some terminal nodes. A strict consensus tree of these trees collapsed for 68 nodes, with the tree length of 353, the Consistency Index (CI) of 0.58, and the Retention Index (RI) of 0.95.

The implied weighting (IW) analysis with a *K*-value of 28.183594 (calculated by the script setk.run) generated five most parsimonious trees. These trees are largely congruent in topology, but inconsistent regarding some terminal nodes. The strict consensus tree (Figs. 14–16) of these trees collapsed for 68 nodes, with the tree length of 351, CI of 0.58, and RI of 0.95. The topology is basically identical to that of the EW analysis. The following description of the cladogram is based on the consensus tree under IW.

Panorpidae

A sister group-relationship between Panorpidae and Panorpodidae (Fig. 14) is very highly supported (BS = 99, BR = 4) by four synapomorphies 12:1 (Fig. 3B), 14:1 (Fig. 3B), 19:1,2 (Fig. 3B, C), and 31:1 (Fig. 4B, C). The monophyly of Panorpidae is maximally supported (BS = 100, BR = 14) by 13 synapomorphies 1:1 (Fig. 1I), 3:2 (Fig. 1E), 6:1 (Fig. 2C), 7:1 (Fig. 2C), 15:1 (Fig. 3C), 23:1 (Fig. 2C), 26:1 (Fig. 4C), 36:1 (Fig. 4C), 48:1 (Fig. 4C), 57:1 (Fig.4C), 135:1 (Fig. 10C), 165:1 (Fig. 12C), and 166:1 (Fig. 13E).

Neopanorpinae ***subfam.n.***

The monophyly of Neopanorpinae **subfam.n.** (Fig. 14; description below) is very highly supported (BS = 98, BR = 9) by six synapomorphies 4:1 (Fig. 1K), 9:1 (Fig. 2I); 16:1 (Fig. 3D), 18:1 (Fig. 3D), 32:1 (Fig. 5J), and 33:1 (Fig. 5J, K). In Neopanorpinae, the topology of five clades is supported as follows: the *N. denticulata* group + (the *N.*

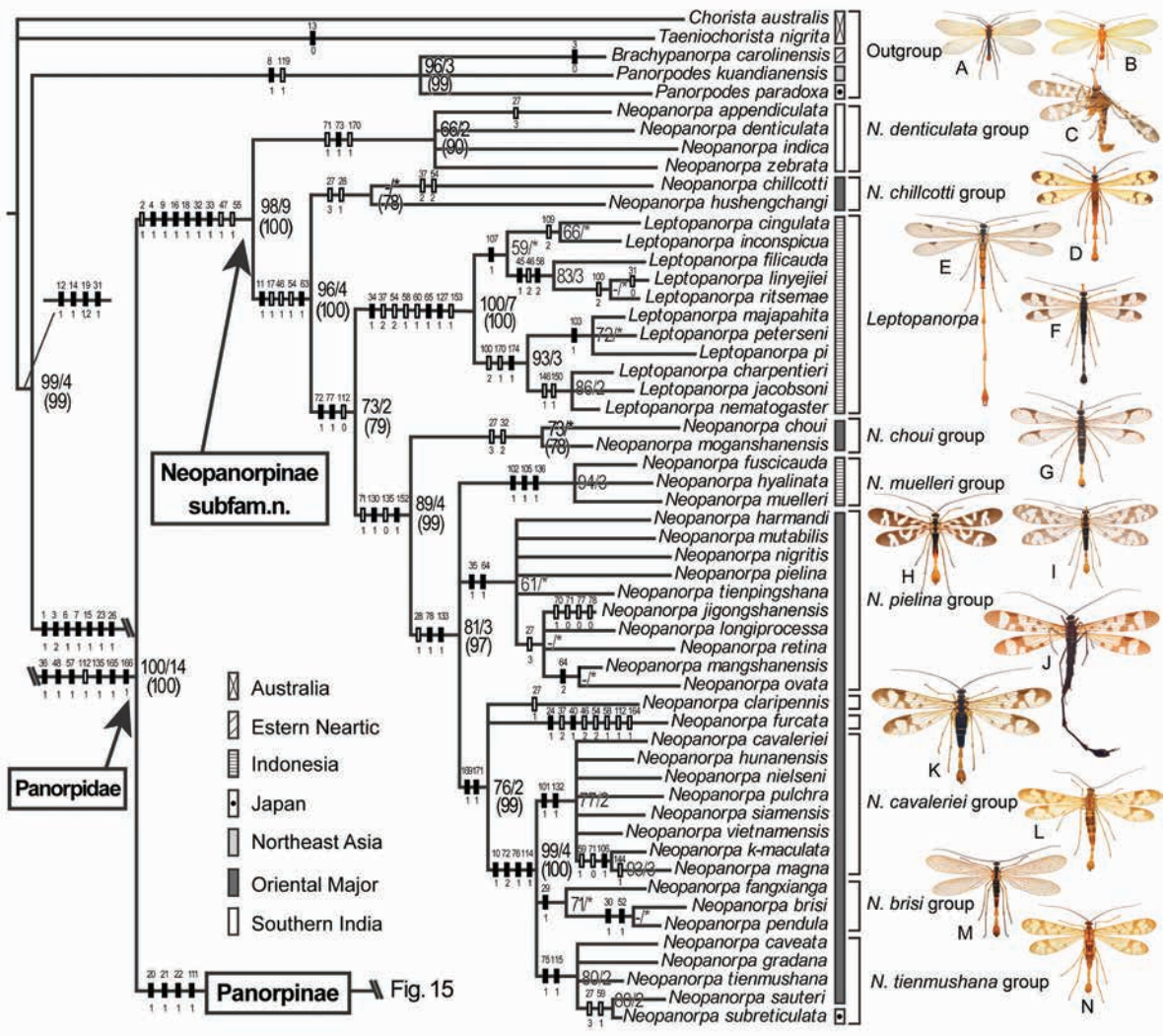

Fig. 14. Strict consensus tree (part I) obtained under implied weighting (IW). Non-homoplasious synapomorphies are indicated by closed squares and homoplasies by open squares. Bootstrap value (BS, shown as '-' if smaller than 50) and Bremer support values (BR, shown as '*' if smaller than 2) are separated by a slash '/' and marked at the right side of each node. Ultrafast Bootstrap values (UFBS, in brackets) are marked below BS and BR, and omitted at some terminal nodes due to inconsistent topologies. Distributional information is marked on the right side of the taxa names. 'Northeast Asia' refers to northeastern China, Russian Far East, and North and South Korea. 'Oriental Major' refers to the Oriental Region excluding India, Indonesia and Japan. Male habitus are marked along the tree on the right side (not to scale). (A) *T. nigrita* Riek; (B) *Po. paradoxa* MacLachlan; (C) *N. denticulata* Rust & Byers; (D) *N. chillcotti* Byers; (E) *L. linyejiei* Wang & Hua; (F) *L. peterseni* Lieftinck; (G) *N. muelleri* (van der Weele); (H) *N. harmandi* (Navás); (I) *N. longiprocessa* Hua & Chou; (J) *N. furcata* (Hardwicke); (K) *N. cavaleriei* (Navás); (L) *N. vietnamensis* Willmann; (M) *N. brisi* (Navás); (N) *N. tienmushana* Cheng. [Colour figure can be viewed at wileyonlinelibrary.com].

chillcotti group + [*Leptopanorpa* + the remaining species of *Neopanorpa*]), indicating the paraphyly of the genus *Neopanorpa*.

The genus *Leptopanorpa* is maximally supported (BS = 100, BR = 7) by three synapomorphies 34:1 (Fig. 5J), 65:1 (Fig. 9B), and 127:1 (Fig. 11D–F), and is further split into four subclades.

The *N. denticulata* group is moderately supported (BS = 66, BR = 2) by one synapomorphy 73:1 (Fig. 8A, B). The *N. chillcotti* group is weakly supported by two homoplasies. Excluding the *N. denticulata* and *N. chillcotti* groups, *Leptopanorpa* + the remaining species of *Neopanorpa* are moderately supported (BS = 73, BR = 2) by two synapomorphies 72:1 (Fig. 9J) and 77:1 (Fig. 9K). The remaining species of *Neopanorpa* are highly supported (BS = 89, BR = 4) by two synapomorphies 130:1 (11H) and 152:1 (Fig. 11G).

Panorpinae

The monophyly of Panorpinae (Fig. 15) is moderately supported (BS = 62, BR = 3) by four synapomorphies: 20:1 (Fig. 3I), 21:1 (Fig. 3I), 22:1 (Fig. 3I), and 111:1 (Fig. 10C).

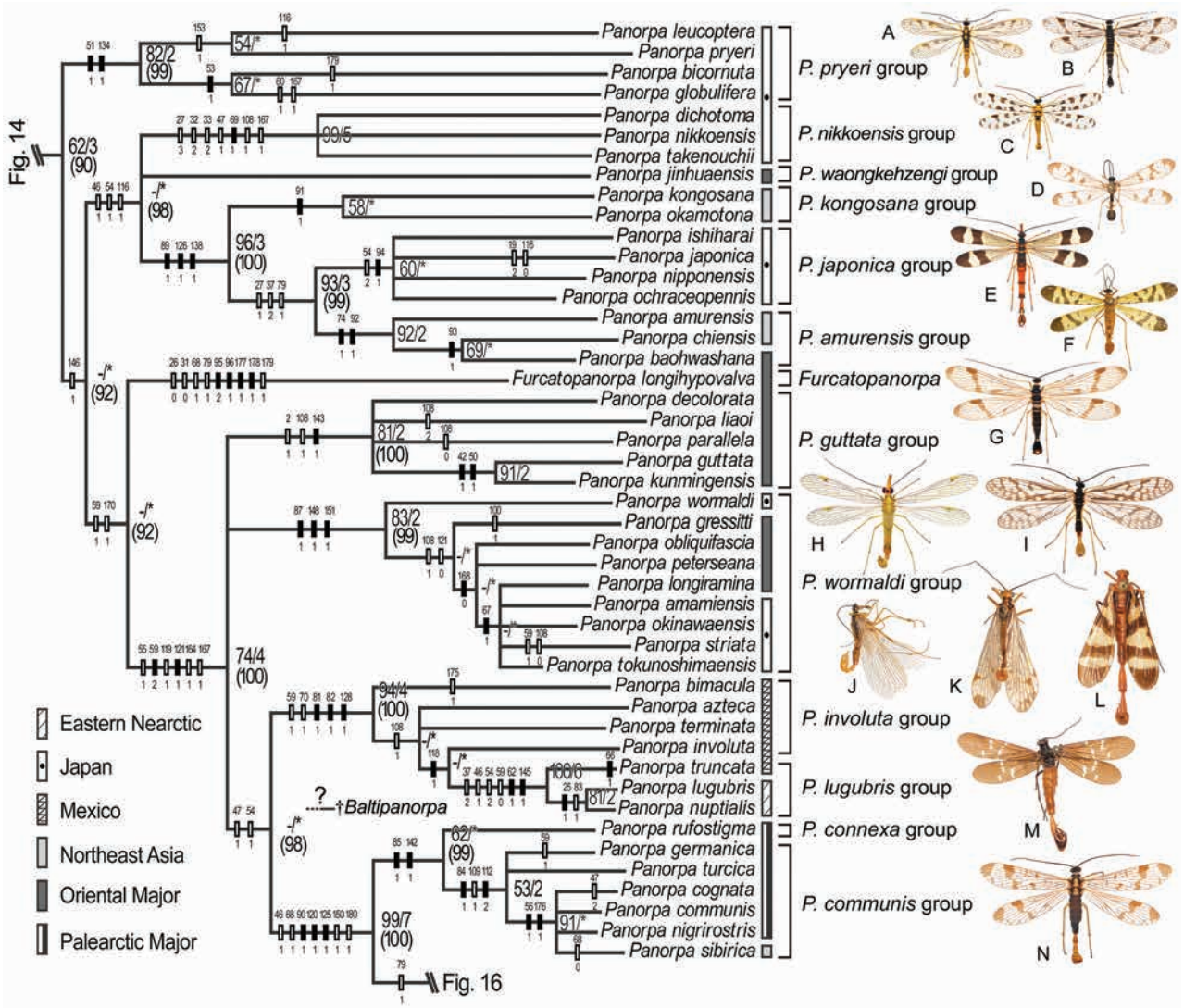

Fig. 15. Strict consensus tree (part II) obtained under IW. †*Baltipanorpa* is marked along the tree with a presumptive position. (A) *P. leucoptera* Uhler; (B) *P. bicornuta* MacLachlan; (C) *P. takenouchii* Miyaké; (D) *P. okamotona* Issiki; (E) *P. japonica* Thunberg; (F) *P. amurensis* MacLachlan; (G) *F. longihypovalva* (Hua & Cai); (H) *P. guttata* Navás; (I) *P. striata* Issiki; (J) *P. azteca* Byers; (K) *P. bimacula* Byers; (L) *P. nuptialis* Gerstaecker; (M) *P. lugubris* Swederus; (N) *P. communis* Linnaeus. [Colour figure can be viewed at wileyonlinelibrary.com].

The genus *Panorpa* is almost certainly a paraphyletic group, with the well-supported genera *Cerapanorpa*, *Dicerapanorpa*, *Furcatopanorpa*, *Megapanorpa* and *Sinopanorpa* nested within different subclades.

The *P. pryeri* group is highly supported (BS = 83, BR = 2) to form a monophyletic group by two synapomorphies 51:1 (Fig. 4C) and 134:1 (Fig. 10C), and there is also a weak support for a sister group relationship of this subclade with respect to the remainder of the subfamily and sister to all the other members of Panorpinae. The *P. amurensis*, *P. kongosana*, *P. japonica*, *P. nikkoensis* and *P. waongkehzengi* groups are weakly supported by three homoplasies. The monotypic genus *Furcatopanorpa* is supported by four autapomorphies 95:2 (Fig. 9T), 96:1 (Fig. 9T), 177:1 (Fig. 13P), and 178:1 (Fig. 13P). The *P. guttata* group is highly supported (BS = 81, BR = 2) by one synapomorphy 143:1 (Wang & Hua, 2017, fig. 5). The *P. wormaldi* group is highly supported (BS = 83, BR = 2) by three synapomorphies 87:1, 148:1 and 151:1.

The clade consisting of the *P. involuta* and *P. lugubris* groups is very highly supported (BS = 94, BR = 4) by three synapomorphies 81:1, 82:1 and 128:1. The sister group-relationship is weakly supported for the *P. lugubris* group + *P. involuta* Byers by one synapomorphy 118:1. Therefore, the *P. involuta* group is supported to be paraphyletic. *P. rufostigma* Westwood (a member of the *P. connexa* group) + the *P. communis* group are moderately supported (BS = 62, BR < 2) by two synapomorphies 85:1 and 142:1.

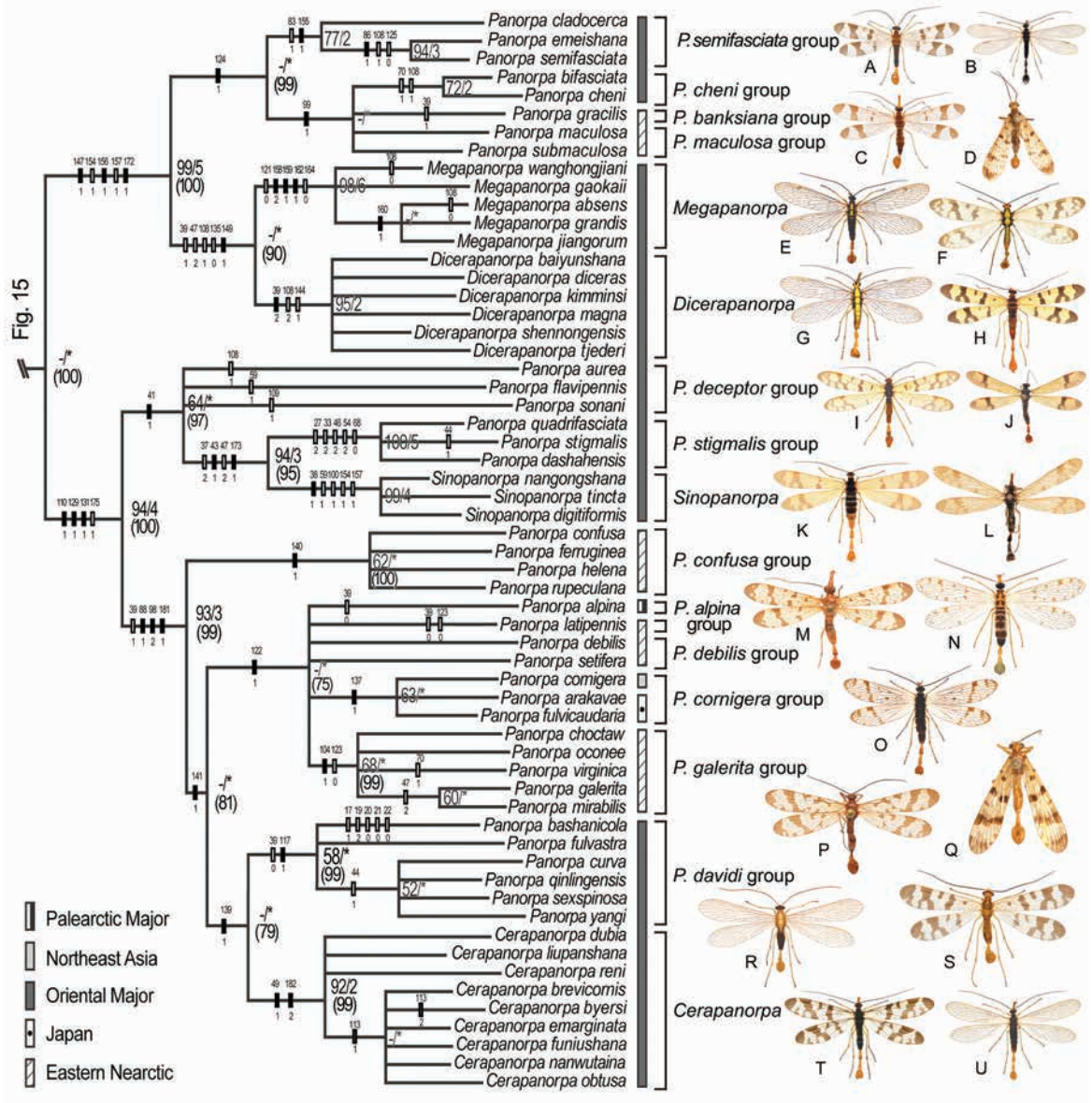

Fig. 16. Strict consensus tree (part III) obtained under IW. (A) *P. cladocerca* Navás; (B) *P. emeishana* Hua, Sun & Li; (C) *P. cheni* Cheng; (D) *P. gracilis* Carpenter; (E) *M. grandis* Wang & Hua; (F) *D. magna* (Chou); (G) *D. diceras* (MacLachlan); (H) *P. aurea* Cheng; (I) *P. dashahensis* Zhou & Zhou; (J) *P. flavipennis* Carpenter; (K) *S. tincta* (Navás); (L) *S. nangongshana* Cai & Hua; (M) *P. confusa* Westwood; (N) *P. alpina* Rambur; (O) *P. cornigera* MacLachlan; (P) *P. galerita* Byers; (Q) *P. oconee* Byers; (R) *P. bashanicola* Hua, Tao & Hua; (S) *P. yangi* Chou; (T) *C. reni* (Chou); (U) *C. obtusa* (Cheng). [Colour figure can be viewed at wileyonlinelibrary.com].

A monophyletic clade (Fig. 16) is very highly supported (BS =99, BR = 5) by three synapomorphies 147:1, 156:1 and 172:1 for the *P. semifasciata* group + (the *P. banksiana* group, the *P. cheni* group and the *P. maculosa* group) + (*Dicerapanorpa* + *Megapanorpa*). The *P. stigmalis* group is maximally supported (BS = 100, BR = 5) by five homoplasies and is sister to *Sinopanorpa*. The *P. confusa* group is moderately supported (BS = 62, BR < 2) by one synapomorphy 140:1. The *P. cornigera*, *P. debilis* and *P. galerita* groups, the *P. alpina* group and *P. latipennis* Hine constitute an unresolved branch supported by one synapomorphy: 122:1. The *P. davidi* group + *Cerapanorpa* are weakly supported by one synapomorphy 139:1.

Maximum likelihood (ML) analysis

The ML analysis generated ten trees (Supporting Information File S2). These trees showed similar topologies with the MP trees, especially the basal split of the two major clades of Panorpidae. The monophyly of Neopanorpinae **subfam.n.**

is maximally supported (UFBS = 100), and the monophyly of Panorpinae is highly supported (UFBS ranges from 85–90). Incongruences of the topologies were mainly found in the relationships among the *P. guttata* group + the *P. wormaldi* group, which are unsupported as sister groups in the MP analyses.

Systematics

Class Insecta Linnaeus, 1758.
Order Mecoptera Packard, 1886.
Suborder Pistillifera Willmann, 1987.
Superfamily Panorpoidea Latreille, 1802.
Family Panorpidae Latreille, 1802.

Key to subfamilies, genera and species groups of Panorpidae

(Modified from Wang & Hua, 2019a)

1. Forewing with 1A usually ending proximal to ORs, only one anal cross-vein a between 1A and 2A; hindwing with anterior ending of a proximal to fork of CuP+1A, cu-a absent (Fig. 3D, E); pretarsal claws with second preapical tooth distinctly larger than others (Fig. 2I, J); male notal organ on T3 greatly developed, more or less exceeding rounded or flat postnotal organ on T4 (Fig. 5A–F, I–N); larvae with shallow furrows on head capsule (**Neopanorpinae subfam.n.**) 2

- Forewing with 1A usually ending distal to ORs, at least two anal cross-veins a between 1A and 2A; hindwing with anterior ending of a distal to fork of CuP+1A, cu-a present (Fig. 3C, I); pretarsal claws with preapical teeth similar in size (Fig. 2H); male notal organ on T3 usually short and flat, postnotal organ on T4 small and acute (Fig. 4C–G, M); larvae lacking shallow furrows on head capsule (Panorpinae). 10

2. Wings broad at base, with ratio of forewing widths at ending of M_4 to 1A < 2; male epandrial lobes absent. . . . . *N. denticulata* group

- Wings relatively narrow at base, with ratio of forewing widths at ending of M_4 to 1A ≥ 2 (Fig. 3D, E); male epandrial lobes present (Fig. 9B, C) 3

3. Male hypovalves with outer margin simple, and unconstricted basally (Fig. 8C). . . . . *N. chillcotti* group

- Male hypovalves with outer margin curled dorsad, and constricted basally (Fig. 9J–M). 4

4. Male abdomen much longer than wings (Fig. 14E, F); A7 and A8 extremely elongated, at least four times as long as wide and twice as long as A5 (Fig. 5F); A9 with an elongated basal stalk (Fig. 8M); epandrium with a terminal projection (Fig. 9B); female medigynium with apodemes of axis curved dorsad (Fig. 13G). . . . . *Leptopanorpa*

- Male abdomen usually less elongated (Fig. 14C, D, G–N); A7 and A8 at most three times as long as wide and twice as long as A5; A9 lacking a distinct basal stalk (Fig. A–L); epandrium lacking a terminal projection (Fig. 9C, D); female medigynium with apodemes of axis simple (Fig. 13H–J). 5

5. Male hypandrial processes absent (Fig. 8E); parameres greatly reduced (Fig. 11G–I). . . . . *N. muelleri* group

- Male hypandrial processes present (Fig. 9J–M); parameres well-developed (Fig. 11A–F, J–S). 6

6. Male T3 with a small tooth-like projection under notal organ (Fig. 5M). . . . . *N. brisi* group

- Male T3 without a projection under notal organ (Fig. 5K). 7

7. Meso- and metanotum with a dark mesal stripe narrower than scutellum (Fig. 2E); epandrial lobes small. . . . . *N. tienmushana* group

- Meso- and metanotum with a dark mesal stripe usually broader than scutellum; epandrial lobes greatly developed (Fig. 9C). 8

8. Male notal organ extremely elongated, exceeding to hind border of A6 (Fig. 5C); postnotal organ depressed with a series of long setae (Fig. 5C). . . . . *N. choui* group

- Male notal organ shorter (Fig. 5B, D, E); postnotal organ greatly developed (Fig. 5K). 9

9. Male T4 with a membranous region on anterior portion (Fig. 5L). . . . . *N. pielina* group

- Male T4 lacking a membranous region of anterior portion. . . . . *N. cavaleriei* group

10. Male notal and postnotal organs greatly elongated, exceeding A7; notal organ with four pairs of long setae subapically; postnotal organ slightly longer than notal organ (Krzemiński & Soszyńska-Maj, 2012, figs. 1, 2, 5). . . . . †*Baltipanorpa*

- Male notal and postnotal organs usually less elongated; notal organ lacking long setae subapically; postnotal organ shorter than notal organ (Figs. 4, 5). 11

11. Maxillary palps lacking a sclerotized ring basal to third segment (Fig. 1R–T); male T7 emarginate at apex (Fig. 4C); dorsal aedeagal valves surrounded by lateral wall formed by ventral valves and dorsal processes (Fig. 10C). . . . . *P. pryeri* group

- Maxillary palps with a sclerotized ring basal to third segment (Fig. 1U, V); male T7 simple (Fig. 4D–K); dorsal aedeagal valves simple (Fig. 10D–R). 12

12. Male T7 usually cylindrical, unconstricted or only slightly constricted at base (Fig. 4C–E). 13

- Male T7 greatly constricted at base (Fig. 4F–K). 20

13. Male epandrium not emarginate or indistinctly emarginate; parameres usually crossed subbasally (Fig. 10D–F, H); female medigynium with poorly developed main plate (Fig. 13K–O). 14

- Male epandrium greatly emarginate apically (Fig. 9G); parameres not crossed subbasally (Fig. 10C, I–R); female medigynium with well-developed main plate (Fig. Figure 13P–Z). 18

14. Male notal organ extremely developed, exceeding apex of A8 (Fig. 4D); hypandrium bearing long setae on apex of basal stalk (Fig. 6D). . . . . *P. nikkoensis* group

- Male notal organ less developed (Fig. C, E–G); hypandrium lacking long setae on apex of basal stalk (Fig. 6C, E–X). 15

15. Male gonostyli shorter than half length of gonocoxites (Fig. 6E). . . . . *P. waongkehzengi* group
- Male gonostyli longer than half length of gonocoxites (Fig. 6F, G). 16

16. Male gonostyli greatly elongated, longer than gonocoxites. . . . . *P. kongosana* group
- Male gonostyli less elongated, approximately as long as gonocoxites. 17

17. Male gonocoxites bearing a subtriangular projection directed caudo-mesad on basal third of inner margin (Fig. 9P); distal half of gonostyli greatly curved dorsad (Fig. 9X); female medigynium with apodemes greatly elongated, longer than main plate (Fig. 13N). . . . . *P. amurensis* group
- Male gonocoxites lacking projection on basal third of inner margin; distal half of gonostyli simple; female medigynium with apodemes concealed in or slightly extending beyond main plate (Fig. 13O). . . . . *P. japonica* group

18. Male notal and postnotal organs absent; median tooth of gonostylus greatly enlarged, serrate on inner margin (Fig. 9T); female medigynium with posterior apex of axis greatly elongated and bifurcated (Fig. 13P). . . . . *Furcatopanorpa*
- Male notal and postnotal organs present (Fig. 4C–G); median tooth of gonostylus simple (Fig. 7B–O); female medigynium with posterior apex of axis short and simple (Fig. 13Q–Z). 19

19. Male lateral processes of aedeagus simple, dorsal processes greatly constricted at base, neck-like; female medigynium lacking a dorsal plate (Fig. 13R). . . . . *P. guttata* group
- Male lateral processes of aedeagus greatly elongated (Fig. 10I), dorsal processes simple; female medigynium bearing a broad dorsal plate (Fig. 13Q). . . . . *P. wormaldi* group

20. Male gonocoxital concavity narrow and shallow, not exceeding to middle of gonocoxites with a subtrapezoidal bottom (Fig. 6J–L); gonocoxites lacking fused lobes on dorsal apex; ventral valves of aedeagus projected ventrad, beak-like (Fig. 10J–L). 21
- Male gonocoxital concavity relatively broad and deep, exceeding middle of gonocoxites with a rounded bottom (Fig. 6M–X); gonocoxites with a pair of fused lobes on dorsal apex (Fig. 9Q); ventral valves of aedeagus simple (Fig. 10M–R). 22

21. Male abdomen relatively short, not exceeding apex of wings (Fig. 15J, K). . . . . *P. involuta* group
- Male abdomen greatly elongated, exceeding apex of wings (Fig. 15L). . . . . *P. lugubris* group

22. Male gonocoxites with a medial spine (Fig. 6M, N). 23
- Male gonocoxites lacking a medial spine (Fig. 6O–X). 24

23. Male gonocoxites lacking or with a less developed terminal plate; parameres usually simple; female medigynium with decorated area of axis simple. . . . . *P. connexa* group
- Male gonocoxites bearing well-developed terminal plate (Fig. 6M); parameres usually bifurcated subapically (Fig. 10M); female medigynium with decorated area of axis greatly enlarged (Fig. 13S). . . . . *P. communis* group

24. Male lateral processes of aedeagus reduced (Fig. 10N); female A9 distinctly wider than A8 (Fig. 12G, I, J); anterior margin of medigynium less sclerotized than posterior portion (Fig. 13T, U). 25
- Male lateral processes well-developed (Fig. 10O, P, R); female A9 approximately as wide as A8; anterior margin of medigynium uniformly sclerotized as posterior portion (Fig. 13V–Z). 30

25. Male aedeagus greatly elongated, with its apex greatly exceeding apex of gonocoxites (Fig. 6P). 26
- Male aedeagus less elongated, with its apex concealed in aedeagal concavity, approximate to apex of gonocoxites, or only slightly exceeding apex of gonocoxites (Fig. 6Q–X). 29

26. Male genitalia with an M-shaped process at joint of two gonocoxites ventrally (Fig. 6O); female T9 with lateral margin greatly curved ventrad and enclosing subgenital plate (Fig. 12H). . . . . *P. semifasciata* group
- Male genitalia lacking an M-shaped process at joint of two gonocoxites (Fig. 6Q–X); female T9 simple (Fig. 12K). 27

27. Male hypovalves extremely narrow, thread-like (Fig. 6R); parameres bifurcated (Fig. 6R). . . . . *P. cheni* group
- Male hypovalves relatively broad and stripe-like; parameres simple. 28

28. Male A6 with a single anal horn on dorsal apex. . . . . *P. banksiana* group
- Male A6 lacking anal horns. . . . . *P. maculosa* group

29. Male A6 with a single anal horn (Fig. 4I); female with laterotergites of A9 greatly elongated, stick-like and fused with medigynium on inner margin (Fig. 12K). . . . . *Megapanorpa*
- Male A6 with a pair of anal horns (Fig. 4K); female with laterotergites short and simple (Fig. 12I). . . . . *Dicerapanorpa*

30. Male A6 beveled at apex (Fig. 4G, H). 31
- Male A6 truncated at apex (Fig. 4I–K). 33

31. Male T6 with a tuft of stout setae dorsally; base of A7 greatly constricted, stalk-like (Fig. 4H). . . . . *Sinopanorpa*
- Male T6 lacking a tuft of stout setae dorsally; A7 usually simple (Fig. 4G). 32

32. Male notal organ on T3 greatly elongated, stick-like, exceeding middle of T4; A6–A8 greatly elongated (Fig. 4G); female axis of medigynium slender (Fig. 13V). . . . . *P. stigmalis* group
- Male notal organ on T3 less elongated, not reaching middle of T4; A6–A8 less elongated; female axis of medigynium stout. . . . . *P. deceptor* group

33. Male dorsal aedeagal processes lacking a swollen membranous process dorso-subapically . . . . . *P. confusa* group
- Male dorsal aedeagal processes with a swollen membranous process dorso-subapically (Fig. 10P–R). 34

34. Male genitalia with aedeagal hamulus present (Figs. 6T, U, 10Q); apical third of dorsal processes simple. 35
- Male genitalia lacking aedeagal hamulus; apical third of dorsal processes greatly curved ventrad (Fig. 10R). . . . 38

35. Male A6 lacking anal horns. . . . . *P. alpina* group
- Male A6 with a single anal horn. 36

36. Male gonostylus with an accessory lobe on ventral surface (Fig. 6V, W); aedeagal hamulus simple and rounded. . . . . *P. galerita* group
- Male gonostylus lacking an accessary lobe; aedeagal hamulus bifurcated and slender (Fig. 10P). 37

37. Male aedeagal hamulus with two branches mostly coalesced (Fig. 10P); dorsal processes bifurcated subapically (Fig. 10P). . . . . *P. cornigera* group
- Male aedeagal hamulus with two branches divergent; dorsal processes simple. . . . . *P. debilis* group

38. Male A6 lacking anal horns; parameres sigmoidally twisted and usually crossed subdistally (Figs. 6X, 10R); female medigynium with ventral plate simple (Fig. 13Y). . . . . *P. davidi* group
- Male A6 with a single anal horn (Fig. 4J); parameres simple (Fig. 7K–O); female medigynium with ventral plate split (Fig. 13Z). . . . . *Cerapanorpa*

Neopanorpinae Wang & Hua, subfam.n.

http://zoobank.org/urn:lsid:zoobank.org:act:091A87BA-A621-48C3-B4B4-974426618393

Type genus: *Neopanorpa* van der Weele, 1909.

Diagnosis. The new subfamily can be differentiated from Panorpinae by the following characters: 1) rostrum relatively slender with lateral margins parallel (Fig. 1K–P); 2) compound eyes enlarged, as wide as or wider than the middle of rostrum (Fig. 1K–P); 3) meso- and metanotum concolorous or frequently with a distinct black mesal stripe (Fig. 2E), and lacking a yellow mesal stripe as in Panorpinae; 4) wings usually narrow at base; forewing with M_{3+4} usually shortened, 1A usually ending proximal to ORs, only one anal cross-vein between 1A and 2A, 3A greatly shortened; hindwing with anterior ending of a proximal to the fork of CuP+1A, 1A straight basally, cu-a absent (Fig. 3D, E); 5) pretarsal claws with second preapical tooth distinctly larger than others (Fig. 2I, J); in males: 6) notal organ on T3 greatly developed, more or less exceeding rounded or flat postnotal organ on T4 (Fig. 5A–N); 7) epandrium usually truncated terminally, usually bearing a pair of epandrial lobes (Fig. 9B–D); 8) paramere usually glabrous (Fig. 11A–S); in females: 9) medigynium usually with poorly developed main plate, and a pair of long twisted posterior arms (Fig. 13E–J); and in larvae (only known for *Neopanorpa*): 10) head capsule with shallow furrows, reduced antennae, shortened setae and flattened compound eyes, and trunk with short dorsal processes (Jiang *et al.*, 2019b).

Genera included. Leptopanorpa MacLachlan, 1875 and *Neopanorpa* van der Weele, 1909.

Distribution. Oriental Region: East, South, and Southeast Asia.

Panorpinae Latreille, 1802

Panorpatae Latreille, 1802: 295; Panorpinae – Enderlein, 1910: 387; Esben-Petersen, 1915: 216; *id*., 1921: 11.

Type genus: *Panorpa* Linnaeus, 1758.

Emended diagnosis. This subfamily can be differentiated from Neopanorpinae **subfam.n.** by the following characters: 1) rostrum stout, tapering towards apex (Fig. 1E–J); 2) compound eyes usually narrower than middle of rostrum (Fig. 1E–J); 3) meso- and metanotum frequently with yellow mesal stripe (Fig. 2C, D) or concolorous; 4) wings broad at base; forewing with M_{3+4} well-developed, 1A usually ending distal to ORs, two (occasionally three) anal cross-veins between 1A and 2A, 3A distinct; hindwing with anterior ending of a distal to the fork of CuP+1A, 1A curved subbasally, cu-a distinct (Fig. 3C, I); 5) pretarsal claws with preapical teeth similar in size (Fig. 2H); in males, 6) notal organ on T3 usually short and flat, postnotal organ on T4 small and acute (Fig. 4C–O); 7) epandrium mostly emarginate at apex, frequently forming a pair of finger-like posterior processes laterally (Fig. 7F, G); 8) parameres usually bearing numerous microtrichia or long spines (Fig. 10C–E); in females, 9) medigynium usually with a well-developed main plate, and a pair of short tapering posterior arms (Fig. 13K–Z); and in larvae (known for all genera except †*Baltipanorpa*): 10) head capsule lacking shallow furrows, with well-developed antennae, setae, and compound eyes, and trunk with long dorsal processes (Chen & Hua, 2011; Wang & Hua, 2019a; Jiang *et al.*, 2019b).

Genera included. Panorpa Linnaeus, 1758, *Sinopanorpa* Cai & Hua, 2008, *Furcatopanorpa* Ma & Hua, 2011, †*Baltipanorpa* Krzemiński & Soszýnska-Maj, 2012, *Dicerapanorpa* Zhong & Hua, 2013, *Cerapanorpa* Gao *et al.*, 2016, and *Megapanorpa* Wang & Hua, 2019.

Distribution. Holarctic and Oriental Regions: Eurasia and North America.

Discussion

Phylogeny of Panorpidae

Based on our present morphological phylogenetic analyses and recent molecular studies (Hu *et al.*, 2015; Miao *et al.*, 2019), the Panorpidae can be divided into two major

clades, Neopanorpinae and Panorpinae. This classification also received supports from the morphology of the egg chorion (Ma *et al.*, 2009), the chromosome number (Miao *et al.*, 2019) and the larval morphology and biology (Jiang *et al.*, 2019b). However, this result differs considerably from the tree inferred mainly from the morphology of the female medigynium by Ma *et al.* (2012), which regarded *Furcatopanorpa* as a sister taxon to all the other genera of Panorpidae. This inconsistence may result from the insufficient taxon sampling and character encoding of the latter phylogenetic analysis.

Based on our present study, the *N. denticulata* group is sister to all the other members in Neopanorpinae (Fig. 14). Species in this group have a broad wing base (11:0) and lack epandrial lobes in male genitalia (63:0), differing from all the other members in Neopanorpinae. This result is inconsistent with recent molecular studies (Hu *et al.*, 2015; Miao *et al.*, 2019), which regard *N. chillcotti* Byers as sister to all the other members in Clade I (= Neopanorpinae). This inconsistence results from the exclusion of the *N. denticulata* group in the previous phylogenetic studies (Hu *et al.*, 2015; Miao *et al.*, 2019). In fact, when excluding the *N. denticulata* group, our study also supports that the *N. chillcotti* group is sister to all the other members in Neopanorpinae.

The Indonesian endemic genus *Leptopanorpa* is nested in the paraphyletic *Neopanorpa*. This result agrees with Miao *et al.* (2019) and Wang & Hua (2020). In our present analyses, *Leptopanorpa* is sister to all the *Neopanorpa* species if the *N. denticulata* and *N. chillcotti* groups are excluded. In this case, to resolve the paraphyly problem of the genus *Neopanorpa*, the *N. denticulata* and *N. chillcotti* groups have to be raised to generic status.

The *P. pryeri* group is supported to be the sister taxon to all the other members in Panorpinae (Fig. 15). Its unique morphological character is the lack of a sclerotized ring basal to the third segment of maxillary palp (Issiki, 1933), (5:0, Fig. 1E–T), which is present in all the other examined species of Panorpidae (5:1, Fig. 1U, V). This sclerotized ring is also absent in the outgroups Choristidae and Panorpodidae (Fig. 1B, Q); thus, we wondered if this group kept some plesiomorphic characters and was sister to all the other members in Panorpidae. Recent molecular phylogenetic analyses, however, suggest that *P. bicornuta* MacLachlan, a member of this group, is either sister to *P. japonica* or to *P. takenouchii* Miyaké (Whiting, 2002; Hu *et al.*, 2015). Therefore, the maxillary ring (5:1, Fig. 1U, V) was likely acquired by the common ancestor of the Panorpidae, but lost in the direct ancestor of the *P. pryeri* group.

The position of the monotypic genus *Furcatopanorpa* is debatable (Fig. 15). *F. longihypovalva* (Hua & Cai) is uniquely identified among Panorpidae by a series of autapomorphies, such as the large heterochromatic blocks in the chromosomes (Miao *et al.*, 2019), the lack of notal and postnotal organs (26:0, 31:0; Fig. 4A), the wide (95:1) and serrate median tooth (96:1) of the male gonostylus (Fig. 9T), and the greatly elongated (177:1) and bifurcated posterior apex of the axis (178:1) in the female medigynium (Fig. 13P). Previously, *Furcatopanorpa* was regarded as a sister taxon to all the other genera of Panorpidae in a morphological analysis (Ma *et al.*, 2012), but merely sister to the *P. guttata* group under MP, or the northeastern Asian species under ML and Bayesian Inference (BI) based on DNA sequence data (Miao *et al.*, 2019). Our results confirm that *Furcatopanorpa* belongs to Panorpinae, in accordance with Hu *et al.* (2015) and Miao *et al.* (2019).

The western Palearctic *P. connexa* group + the *P. communis* group are well-supported to form a monophyletic clade, which is sister to a much larger and complicated clade consisting of *Dicerapanorpa* + *Megapanorpa*, *Cerapanorpa* and the remaining species of *Panorpa* (Fig. 15). Taxonomically, the type species of *Panorpa*, *P. communis* Linnaeus belongs to the western Palearctic clade. Therefore, the *P. communis* group + the *P. connexa* group can possibly be regarded as the *Panorpa* in a narrower sense.

The genus *Sinopanorpa* is sister to the *P. stigmalis* group (Fig. 16), suggesting a potential generic status of the latter. The genus *Cerapanorpa* is sister to the *P. davidi* group (Fig. 16), supporting previous molecular results (Hu *et al.*, 2015; Miao *et al.*, 2019). However, the interspecific relationships are not satisfactorily resolved in *Cerapanorpa* (Figs. 15, 16), probably due to their short divergence history (Miao *et al.*, 2017, 2019; Hu *et al.*, 2019) and great morphological resemblances (Gao *et al.*, 2016; Gao & Hua, 2019) among the congeners. This situation is also present in *Dicerapanorpa*, *Megapanorpa* and *Sinopanorpa*.

In order to resolve the paraphyly of *Panorpa*, two solutions are feasible: (1) lumping a diversity of species groups under only one generic name; and (2) retaining the six established genera, †*Baltipanorpa*, *Cerapanorpa*, *Dicerapanorpa*, *Furcatopanorpa*, *Megapanorpa* and *Sinopanorpa*, and further splitting the paraphyletic *Panorpa* into several additional genera. Our present study appears to support the second solution by recognizing 24 distinct species groups in *Panorpa*. Among them, 15 clades were consistently supported to be monophyletic in both MP and ML analyses, but some groups (*e.g.*, the *P. deceptor* and *P. debilis* groups) received limited support. It appears that the taxon sampling in the present study is insufficient to confidently split the paraphyletic *Panorpa*, which requires further investigation.

Biogeography of the Panorpidae

Origin and early divergence

The origin of Panorpidae dates back to the Early Cretaceous (ca. 122.5 mya) (Miao *et al.*, 2019). The East Asian fauna of Panorpidae exhibits the greatest diversity at the generic and species levels, confirming the Laurasian origin of this family (Byers, 1988; Hu *et al.*, 2015). Specifically speaking, East Asia (including China, Japan, the Korean Peninsula, Russian Far East and adjacent regions) is most likely the origin centre of Panorpidae by harbouring approximately 60% (ca. 300/500) of the species (Penny & Byers, 1979; Wang & Hua, 2017, 2018, 2019a,b) and 66% (21/32) of the species groups. According to Miao *et al.* (2019), the split between Neopanorpinae and Panorpinae are dated to around 54.5–66.0 mya, shortly after the Cretaceous-Paleogene extinction event. The early divergence

of Panorpidae at the subfamilial and generic levels might be correlated to the geographical movements caused by the collision between India and Eurasia (beginning ca. 55.0 mya, Aitchison *et al.*, 2007), and post-collision tectonic movements such as the uplift of the Qinghai-Tibetan Plateau, the orogeny of the Hengduan Mountains, and the extrusion and escape of the Sundaland (Wang & Hua, 2020).

The Oriental fauna

Neopanorpinae is typically an Oriental group (Fig. 17). According to Miao *et al.* (2019), *N. chillcotti* Byers is sister to all the other members in Neopanorpinae and split from the latter 49.1–34.9 mya. Based on our cladistic analysis, however, the *N. denticulata* group likely split from other members earlier than the *N. chillcotti* group. Given the East Asian origin and the relatively weak dispersal ability of the Panorpidae (Byers, 1988; Miao *et al.*, 2017; Hu *et al.*, 2019), the spreading of the common ancestor of the *N. denticulata* group to the Indian subcontinent was unlikely earlier than the collision between India and Eurasia that began 55.0 mya (Aitchison *et al.*, 2007). The Himalayan fauna is heterogeneous by composing the *N. chillcotti* group (ca. 10 spp.) and a few species such as *N. furcata* (Hardwicke) nested in the Chinese and southeast Asian species cluster. The southern Chinese and Mainland Southeast Asian faunas are mixed in Neopanorpinae.

The Indonesian fauna is also heterogeneous by consisting of 14 species of *Leptopanorpa* and several species of *Neopanorpa* (Lieftinck, 1936; Chau & Byers, 1978; Wang & Hua, 2020). By analysing concatenated morphological characters and DNA sequence data, Wang & Hua (2020) speculated that the ancestor of *Leptopanorpa* likely diverged from *Neopanorpa* owing to the vicariance caused by the collision-extrusion tectonics of Sundaland in the Oligocene (33.9–23.0 mya), while the sympatric *N. muelleri* group likely originated somewhere else in the southeastern Asia, and subsequently migrated southward through the exposed Sundaland during the glacial periods in the Neogene (23.0–2.6 mya).

In contrast, the Oriental members of Panorpinae are mostly confined in the temperate and subtropical zones (Fig. 17), with abundant species of *Panorpa* in southern China, and five genera (*Cerapanorpa*, *Dicerapanorpa*, *Furcatopanorpa*, *Megapanorpa* and *Sinopanorpa*) endemic to China. Only two species are recorded from the Southeast Asia: *P. malaisei* Byers from northeastern Myanmar (Byers, 1999) and *P. auripennis* Bicha from northern Thailand (Bicha, 2019).

The Japanese fauna

Japan is notable for its high species diversity and endemism in a relatively smaller land mass compared with the mainland Asia (Myers *et al.*, 2000; Tojo *et al.*, 2017). In Neopanorpinae, only one species, *N. subreticulata* Miyamoto & Makihara has been reported from Japan's southernmost Ryukyu Islands. This species closely resembles *N. sauteri* (Esben-Petersen) from Taiwan, China by an extremely elongated male notal organ and other features (Miyamoto & Makihara, 1979), indicating their short divergence history.

In contrast, the Japanese fauna of Panorpinae is abundant and consists of ca. 32 endemic species in five species groups (Miyaké, 1908, 1910, 1911, 1913; Issiki, 1933; Miyamoto, 1977, 1978, 1984, 1985; Miyamoto & Nakamura, 2008; Nakamura, 2009): the *P. pryeri* group (5 spp. endemic to Japan), the *P. nikkoensis* group (4 spp. endemic to Japan), the *P. japonica* group (10 spp. in Japan and 1 sp. in southern China), the *P. wormaldi* group (9 spp. in Japan and 8 spp. in southern China), and the *P. cornigera* group (4 spp. in Japan and 1 sp. in mainland Northeast Asia). These species groups are dispersed on the phylogenetic tree, indicating that they are unlikely descendants of an indigenous Japanese ancestor, but derived instead from several different ancestors that migrated from mainland Asia to Japan.

We speculate that at least five dispersal events (Fig. 17) might have occurred for the Japanese fauna, inferred correspondingly from five distinct clades (Figs. 14–16): 1) the *P. pryeri* group; 2) the *P. nikkoensis* and *P. japonica* groups, which are mixed with the mainland Asian *P. waongkehzengi* (ca. 5 spp.), *P. amurensis* (ca. 6 spp.) and *P. kongosana* groups (2 spp.); 3) the *P. wormaldi* group; 4) the *P. cornigera* group; and 5) *N. subreticulata*. According to the divergence time estimated by Miao *et al.* (2019), most groups of *Panorpa* migrated northeastward from southern China through exposed land bridges to Japan in the Eocene. In contrast, the *P. cornigera* group likely migrated southeastward from northeastern Asia by way of the Korean Peninsula to enter Japan in the Miocene. *N. subreticulata* is likely the last arrival, which colonized the Kyushu Islands by way of Taiwan after the Miocene.

The *P. amurensis* group is closely related to the *P. japonica* group (Fig. 15). It probably originated from Japan, and dispersed into Northeast Asia by way of the Korean Peninsula (Fig. 17), with only one species, *P. baohwashana* Cheng inhabiting eastern China. A puzzling species, *P. kellogi* Cheng from Fujian, China, bears a series of protuberances on the inner margin of the male gonostylus (94:1), and slender and uncrossed male parameres (116:0) (Cheng, 1957a), implying its close relationship to *P. japonica*. Speculatively, *P. kellogi* and *P. japonica* shared a direct common ancestor that migrated southwestward from Japan to Fujian, China through exposed landmass during a cold glacial period, and later separated in a warm interglacial period due to the rising sea level. Similarly, such a range shifting between southeastern China and Japan was also estimated for a stag beetle and a caddisfly (Tojo *et al.*, 2017).

The western Palearctic fauna

The *P. communis* group (ca. 19 spp.) + the *P. connexa* group (5 spp.), and the *P alpina* group (represented by *P. alpina* Rambur) constitute the western Palearctic fauna of *Panorpa* (Willmann, 1977). According to Miao *et al.* (2019), *P. rufostigma* (a member of the *P. connexa* group) + the *P. communis* group forms a monophyletic clade and split from the main Asian fauna in the Eocene, while *P. alpina* is distantly grouped with several Chinese species and split from the main Asian fauna in the Oligocene. Correspondingly, in our present study, *P. rufostigma* + the *P. communis* group are highly supported to form

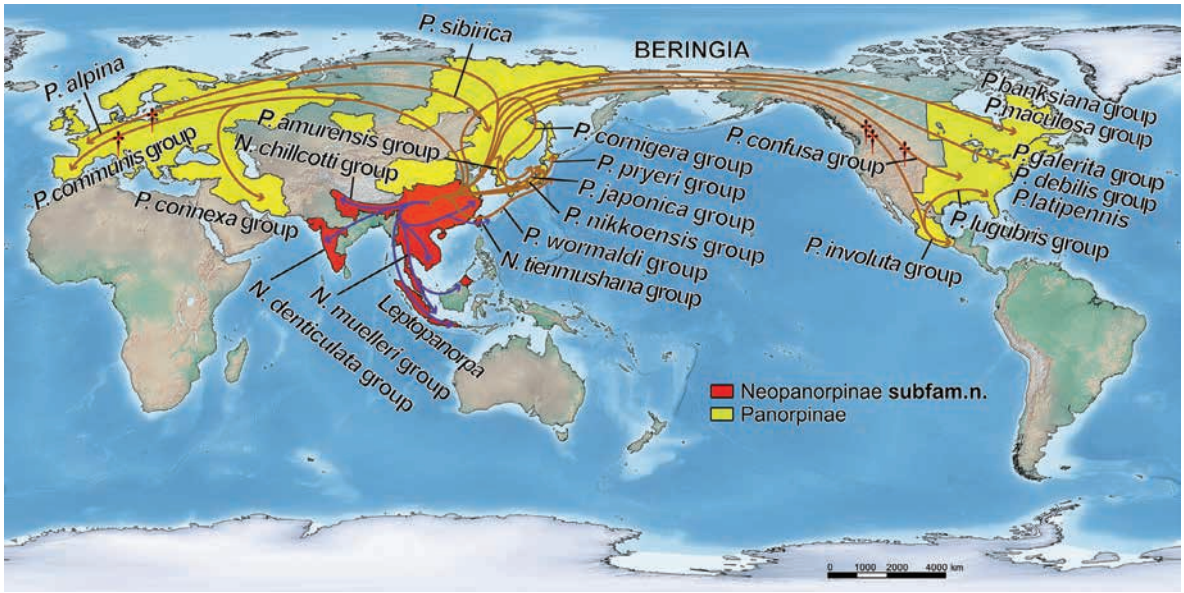

Fig. 17. Distributional range and putative dispersal routes of Panorpidae. Countries with distributional records are fully coloured, except that some large ones are coloured at the provincial/state level. Tibet, China is only coloured at the Himalayas. Arrowed lines show the putative dispersal routes for some species or species groups. Dagger symbol '†' indicates fossil localities. [Colour figure can be viewed at wileyonlinelibrary.com].

a monophyletic clade (Fig. 15), distantly related to *P. alpina* (Fig. 16). These facts congruently support the heterogeneity of the western Palearctic fauna of *Panorpa*, and suggest that two Asia-Europe dispersal events might have occurred independently for the western Palearctic fauna. Alternatively, these two lineages are likely descendants of different Asian ancestors that migrated westward to Europe, instead of deriving from an indigenous European ancestor (Fig. 17).

P. sibirica Esben-Petersen, a single Palearctic species penetrated into Northeast Asia (Martynova, 1957), very likely had a European ancestor that reversely migrated eastward from Europe through Siberia to Northeast Asia (Fig. 17), and genetically separated from its European relatives in the Miocene (Miao *et al.*, 2019).

The Nearctic fauna

In the Holarctic Region, a disjunct distribution of closely related organisms between Eurasia and North America is a common biogeographic pattern (Mikkola *et al.*, 1991; Sanmartin *et al.*, 2001; von Dohlen *et al.*, 2002). Beringia, once exposed as a large landmass and covered with mesic forest during the ice ages, was most likely the corridor for the faunal interchange between these two realms (Downes & Kavanaugh, 1988; Vila *et al.*, 2011; Jiang *et al.*, 2019a). Evidently, Beringia was formed (although partially submerged at some stages) at the end of the Early Cretaceous (ca. 100.0 mya) and once covered with thermophilous palaeoflora (Zakharov *et al.*, 2011), providing an ideal pathway for scorpionflies to disperse from East Asia to North America. Considering the Asian origin of Panorpidae, the ancestor of the Nearctic scorpionflies probably migrated eastward by way of Beringia during the Eocene or Oligocene (Byers, 1988; Downes & Kavanaugh, 1988). Fossil records imply that *Panorpa* entered the Nearctic Region no later than the Early Eocene, and once inhabited the western and central North America (Fig. 17; Scudder, 1890; Cockerell, 1907; Archibald *et al.*, 2013). Subsequently, they perished in most parts of the western and central North America owing to the drying climate and declining forests during the Miocene-Pliocene transition (7.0–5.0 mya, Axelrod, 1985). However, *P. nuptialis* Gerstaecker in the *P. lugubris* group likely adapted the dry climate, and can be found from cultivated fields, pastures, and dry open woods in southern U.S.A. and northern Mexico (Esben-Petersen, 1921; Byers, 1963).

Four major lineages of the Nearctic species were revealed in our present analysis (Figs. 15, 16), indicating that four dispersal events might have occurred separately for this fauna. The first lineage consists of the paraphyletic *P. involuta* (ca. 30 spp.) and the monophyletic *P. lugubris* groups (4 spp.). Our results support Byers's (1988) assumption that the *P. lugubris* group likely originated from a Mexican ancestor, which dispersed to southeast U.S.A. during a warm interglacial period and separated from the main Mexican fauna owing to the cooling climate in a subsequent glacial period. The second lineage comprises the *P. banksiana* (4 spp., represented by *P. gracilis* Carpenter) and *P. maculosa* groups (2 spp.). The third lineage is the *P. confusa* group (ca. 30 spp.). The last and fourth lineage consists of the *P. debilis* (7 spp.) and the *P. galerita* groups (ca. 10 spp.), and *P. latipennis*.

Based on our present study, the aedeagal hamulus (122:1) is a synapomorphy shared by a wide range of species from Europe (the *P. alpina* group), northeast Asia (the *P. cornigera* group) and North America (the *P. debilis* group, the *P. galerita* group, and *P. latipennis*) (Fig. 16). However, some hamulus-bearing species diverged in different clades in the molecular analyses

(Hu *et al.*, 2015; Miao *et al.*, 2019), suggesting a possible convergent evolution of the hamulus. Further research is needed to decipher whether the hamulus was acquired by their direct common ancestor, or independently evolved several times among these species.

Systematic position of the fossil species

Up to date, no fossil species have ever been reported for Neopanorpinae. The monotypic genus †*Baltipanorpa* can be readily recognized as a member of Panorpinae by the following characters: in the forewings, 1A ending beyond ORs (17:0), three anal cross-veins (19:1); and in the hindwings, anterior ending of a distal to the fork of CuA + 1A (21:1), 1A curved at a (22:1) and cu-a distinct (20:1) (Krzemiński & Soszyńska-Maj, 2012, figs. 3, 4, CuA, CuP, 1A and 2A marked as CuP, 1A–3A in fig. 4B). The basally constricted A7 (47:1) and elongated A8 (54:1) possibly indicates that it belonged to a more distal lineage instead of an earlier branching one in Panorpinae, because most early-branching groups in this subfamily bear unconstricted A7 (47:0) and unelongated A8 (54:0). By some autapomorphies such as the greatly elongated male postnotal organ, †*Baltipanorpa* likely represents a collateral, terminated branch that left no extant descendants in Panorpinae.

Only seven extinct species were described in *Panorpa* from the Eocene to Oligocene Europe and North America (Scudder, 1890; Cockerell, 1907; Statz, 1936; Carpenter, 1954; Willmann, 1976). The earliest known fossil *Panorpa* was reported from the Early Eocene (52.90 ± 0.83 mya) of MacAbee, Canada (Archibald *et al.*, 2013). This unnamed specimen bears a basally constricted A7 in males. †*P. obsoleta* Carpenter from Baltic amber is similar to the extant *P. communis* group by the short and basally constricted male A7 and A8, and a globular genital bulb (Carpenter, 1954). †*P. rigida* Scudder from Florissant bears a pair of slender posterior arms and a pair of apodemes of axis in the female medigynium (Willmann, 1989), superficially similar to the extant Nearctic *P. confusa* group.

The earliest known fossil *Panorpa* from the Early Eocene (Archibald *et al.*, 2013) was used to calibrate the most recent ancestor of Panorpinae by Miao *et al.* (2019). In the light of the East Asian origin of Panorpidae, however, this fossil *Panorpa* was unlikely the common ancestor of Panorpinae, but merely an ancestor or sibling to the present Nearctic species. In other words, this fossil *Panorpa* was likely closer to the tip than to the base of Panorpinae, implying that the diversification time ca. 53.0 mya of Panorpinae was estimated more or less imprecisely due to the 'push towards the present' effect (Giribet, 2015). Further investigations of fossil species and a taxonomic revision of *Panorpa* are needed for tracing a more accurate evolutionary history of Panorpidae.

Conclusions

Our present results overall agree with the recent molecular phylogenetic studies, deepening the understanding of the phylogeny of Panorpidae by applying more comprehensive morphological characters (182) and more representative taxa (155 extant species in eight genera). Our results support the following conclusions: 1) Panorpidae can be categorized into two major clades, Neopanorpinae and Panorpinae; 2) *Panorpa* and *Neopanorpa* are reconfirmed to be paraphyletic groups, with 32 species groups (24 in *Panorpa* and eight in *Neopanorpa*) recognized; 3) the *N. denticulata* and *N. chillcotti* groups likely merit generic status; 4) the monophyly of *Cerapanorpa*, *Dicerapanorpa*, *Megapanorpa*, and *Sinopanorpa* is supported; and 5) Panorpidae likely originated from East Asia, and the independent dispersal events very likely occurred at least twice for the Indonesian fauna, five times for the Japanese fauna, twice for the western Palearctic fauna and four times for the Nearctic fauna.

Supporting Information

Additional supporting information may be found online in the Supporting Information section at the end of the article.

Table S1. List of investigated taxa and related information in the phylogenetic analyses.

File S1. Character matrix.

File S2. Maximum Likelihood trees with Ultrafast Bootstrap values.

Acknowledgements

We are indebted to Pavel Chvojka and David Král (NMCZ), Toshiya Hirowatari and Satoshi Kamitani (KYSU), Li Chen and Zhu Li (ISWU), Hong Pang and Bing-Lan Zhang (SYSU), Xing-Min Wang (SCAU), Jian-Yue Qiu, Cheng-Bin Wang and Hao Xu (MYNU), Shinji Yano (OMGM), Li-Zhen Li and Zi-Wei Yin (SHNU), Xing-Yue Liu and Yu-Chen Zheng (ECAU), and the late George W. Byers (EDKU) for arranging the exchanging, examination and loan of the specimens. We also thank Yuan-Fang Gu, Ye-Jie Lin, Yuan Hua, and Xiao Wang for great help to the first author in the field surveys, Yi-Jun Chai, Wen-I Chou, Lu Jiang, Ri-Xin Jiang, Zhuo-Heng Jiang, Kai Gao, Kai-Wen Gao, Gui-Qiang Huang, Ning Li, Tao Li, Lu Liu, Zhen-Hua Liu, Ying Miao, and Shuang Xue for collecting and donating specimens, Gui-Lin Hu and Meng Wang for loaning specimens, Finks Bakrie, Sepni Juhansah, Imamu Laripin, Rebing Pusadan, and Aris Risyana (Indonesia) for sharing precious information about the insects, Dalton de Souza Amorim (Brazil), Vladimir N. Makarkin, Valeriy I. Shchurov (Russia), Takeyuki Nakamura, and Tomoya Suzuki (Japan) for providing hardly accessible articles, and Xuan-Kun Li for his assistance in the data analysis. Special thanks go to three anonymous reviewers for their valuable comments on the revision of the manuscript. This research was funded by the National Natural Science Foundation of China (Grant numbers 31672341 and 31172125), and the Starting Foundation for the High-level Talents, Dali University (Grant number KY2096124040). The authors declare that there are no conflicts of interest.

Data availability statement

The data that supports the findings of this study are available in the supplementary material of this article, and are openly available in TreeBASE at http://purl.org/phylo/treebase/phylows/study/TB2:S27458, reference number 27458.

References

Aitchison, J.C., Ali, J.R. & Davis, A.M. (2007) When and where did India and Asia collide? *Journal of Geophysical Research*, **112**, B05423. https://doi.org/10.1029/2006JB004706.

Archibald, S.B., Mathewes, R.W. & Greenwood, D.R. (2013) The Eocene apex of panorpoid scorpionfly family diversity. *Journal of Paleontology*, **87**, 677–695. https://doi.org/10.1666/12-129.

Axelrod, D.I. (1985) Rise of the grassland biome, Central North America. *The Botanical Review*, **51**, 163–201.

Beutel, R.G. & Baum, E. (2008) A longstanding entomological problem finally solved? Head morphology of *Nannochorista* (Mecoptera, Insecta) and possible phylogenetic implications. *Journal of Zoological Systematics and Evolutionary Research*, **46**, 346–367. https://doi.org/10.1111/j.1439-0469.2008.00473.x.

Beutel, R.G. & Friedrich, F. (2019) Nannomecoptera and Neomecoptera. *Handbook of Zoology*, pp. 1–161. De Gruyter, Berlin. https://doi.org/10.1515/9783110272543.

Bicha, W.J. (2018) Biodiversity of Mecoptera. *Insect Biodiversity: Science and Society, II* (ed. by R.G. Foottit and P.H. Adler), pp. 705–720. John Wiley & Sons, Hoboken, New Jersey. https://doi.org/10.1002/9781118945582.ch23.

Bicha, W.J. (2019) Scorpionflies (Mecoptera: Panorpidae) collected during project Tiger with the description of three new species from Thailand. *The Pan-Pacific Entomologist*, **95**, 49–63. https://doi.org/10.3956/2019-95.2.49.

Boudinot, B.E. (2018) A general theory of genital homologies for the Hexapoda (Pancrustacea) derived from skeletomuscular correspondences, with emphasis on the Endopterygota. *Arthropod Structure & Development*, **47**, 563–613. https://doi.org/10.1016/j.asd.2018.11.001.

Bremer, K. (1994) Branch support and tree stability. *Cladistics*, **10**, 295–304. https://doi.org/10.1006/clad.1994.1019.

Byers, G.W. (1963) The life history of *Panorpa nuptialis* (Mecoptera: Panorpidae). *Annals of the Entomological Society of America*, **56**, 142–149. https://doi.org/10.1093/aesa/56.2.142.

Byers, G.W. (1965) Families and genera of Mecoptera. *Proceedings of the XII International Congress of Entomology. Section 1*, Systematics, London, p. 123.

Byers, G.W. (1988) Geographic affinities of the North American Mecoptera. *Memoirs of the Entomological Society of Canada*, **120**, 25–30. https://doi.org/10.4039/entm120144025-1.

Byers, G.W. (1993) Antumnal Mecoptera of Southeastern United States. *The University of Kansas Science Bulletin*, **55**, 57–96. https://doi.org/10.5962/bhl.part.773.

Byers, G.W. (1996) Descriptions and distributional records of American Mecoptera. IV. *University of Kansas Science Bulletin*, **55**, 519–547. https://doi.org/10.5962/bhl.part.782.

Byers, G.W. (1999) Thirteen new Panorpidae (Mecoptera) from northern Burma. *Entomologica Scandinavica*, **30**, 197–218. https://doi.org/10.1163/187631200X00246.

Carpenter, F.M. (1931) Revision of the Nearctic Mecoptera. *Bulletin of the Museum of Comparative Zoology*, **72**, 205–277. https://doi.org/10.2307/20023217.

Carpenter, F.M. (1938) Mecoptera from China, with descriptions of new species. *Proceedings of the Entomological Society of Washington*, **40**, 267–281.

Carpenter, F.M. (1954) The Baltic amber Mecoptera. *Psyche*, **61**, 31–40. https://doi.org/10.1155/1954/80512.

Chau, H.C. & Byers, G.W. (1978) The Mecoptera of Indonesia: genus *Neopanorpa*. *University of Kansas Science Bulletin*, **51**, 341–405.

Chen, H.-M. & Hua, B.-Z. (2011) Morphology and chaetotaxy of the first instar larva of the scorpionfly *Sinopanorpa tincta* (Mecoptera: Panorpidae). *Zootaxa*, **2897**, 18–26. https://doi.org/10.11646/zootaxa.2897.1.2.

Cheng, F.Y. (1957a) Descriptions of new Panorpidae (Mecoptera) in the collection of the California Academy of Sciences. *Memoirs of College of Agriculture, National Taiwan University*, **5**, 27–33.

Cheng, F.Y. (1957b) Revision of the Chinese Mecoptera. *Bulletin of the Museum of Comparative Zoology at Harvard College*, **116**, 1–118. https://doi.org/10.1086/402863.

Cockerell, T.D.A. (1907) Some old world types of insects in the Miocene of Colorado. *Science*, **26**, 446–447.

Ding, H., Shih, C.-K., Bashkuev, A., Zhao, Y.-Y. & Ren, D. (2014) The earliest fossil record of Panorpidae (Mecoptera) from the middle Jurassic of China. *ZooKeys*, **432**, 79–92. https://doi.org/10.3897/zookeys.431.7561.

von Dohlen, C.D., Kurosu, U. & Aoki, S. (2002) Phylogenetics and evolution of the eastern Asian-eastern north American disjunct aphid tribe, Hormaphidini (Hemiptera: Aphididae). *Molecular Phylogenetetics and Evolution*, **23**, 257–267. https://doi.org/10.1016/S1055-7903(02)00025-8.

Downes, J. & Kavanaugh, D. (1988) Origins of the North American insect fauna. *The Memoirs of the Entomological Society of Canada*, **120**, 1–11. https://doi.org/10.4039/entm120144fv.

Enderlein, G. (1910) Über die Phylogenie und die Klassifikation der Mecopteren unter Berücksichtigung der fossilen Formen. *Zoologischer Anzeiger*, **35**, 385–399.

Esben-Petersen, P. (1915) A synonymic list of the order Mecoptera together with descriptions of new species. *Entomologiska Meddelelser*, **10**, 216–242.

Esben-Petersen, P. (1921) Mecoptera. Monographic revision: collections zoologiques du Baron Edm. de Selys Longchamps. *Catalogue Systématique et Descriptif*, **5**, 1–172.

Felsenstein, J. (1985) Phylogenies and the comparative method. *The American Naturalist*, **125**, 1–15. https://doi.org/10.1086/284325.

Gao, K. & Hua, B.-Z. (2019) Revision of the genus *Cerapanorpa* (Mecoptera: Panorpidae) with descriptions of four new species. *European Journal of Taxonomy*, **537**, 1–23. https://doi.org/10.5852/ejt.2019.537.

Gao, C., Ma, N. & Hua, B.-Z. (2016) *Cerapanorpa*, a new genus of Panorpidae (Insecta: Mecoptera) with descriptions of three new species. *Zootaxa*, **4158**, 93–104. https://doi.org/10.11646/zootaxa.4158.1.5.

Giribet, G. (2015) Morphology should not be forgotten in the era of genomics–a phylogenetic perspective. *Zoologischer Anzeiger*, **256**, 96–103. https://doi.org/10.1016/j.jcz.2015.01.003.

Goloboff Pablo A., Farris James S. & Nixon Kevin C. (2008) TNT, a free program for phylogenetic analysis. *Cladistics*, **24** , 774–786. http://dx.doi.org/10.1111/j.1096-0031.2008.00217.x.

Goloboff, P.A. & Catalano, S.A. (2016) TNT version 1.5, including a full implementation of phylogenetic morphometrics. *Cladistics*, **32**, 221–238.

Grimaldi, D. & Engel, M.S. (2005) Antliophora: scorpionflies, fleas, and true flies. *Evolution of the Insects*, pp. 468–547. Cambridge University Press, New York, New York.

Hoang, D.T., Chernomor, O., von Haeseler, A., Minh, B.Q. & Vinh, L.S. (2018) UFBoot2: improving the ultrafast bootstrap approximation.

Molecular Biology and Evolution, **35**, 518–522. https://doi.org/10.1093/molbev/msx281.

Hu, G.-L. & Hua, B.-Z. (2020) Review of the scorpionfly genus *Dicerapanorpa* Zhong & Hua (Mecoptera: Panorpidae), wuth descriptions of two new species. *European Journal of Taxonomy*, **711**, 1–13. https://doi.org/10.5852/ejt.2020.711.

Hu, G.-L., Yan, G., Xu, H. & Hua, B.-Z. (2015) Molecular phylogeny of Panorpidae (Insecta: Mecoptera) based on mitochondrial and nuclear genes. *Molecular Phylogenetics and Evolution*, **85**, 22–31. https://doi.org/10.1016/j.ympev.2015.01.009.

Hu, G.-L., Gao, K., Wang, J.-S., Hebert, P.D.N. & Hua, B.-Z. (2019) Molecular phylogeny and species delimitation of the genus *Dicerapanorpa* (Mecoptera: Panorpidae). *Zoological Journal of the Linnean Society*, **187**, 1173–1195. https://doi.org/10.1093/zoolinnean/zlz059.

Hua, Y., Tao, S.-H. & Hua, B.-Z. (2018) An enigmatic new species of *Panorpa* Linnaeus from the Bashan Mountains (Mecoptera, Panorpidae). *ZooKeys*, **777**, 109–118. https://doi.org/10.3897/zookeys.777.26056.

Hünefeld, F. & Beutel, R.G. (2005) The sperm pumps of Strepsiptera and Antliophora (Hexapoda). *Journal of Zoological Systematics and Evolutionary Research*, **43**, 297–306. https://doi.org/10.1111/j.1439-0469.2005.00327.x.

Issiki, S. (1933) Morphological studies on the Panorpidae of Japan and adjoining countries and comparison with American and European forms. *Japanese Journal of Zoology*, **4**, 315–416.

Jiang, D.-C., Klaus, S., Zhang, Y.-P., Hillis, D.M. & Li, J.-T. (2019a) Asymmetric biotic interchange across the Bering land bridge between Eurasia and North America. *National Science Review*, **6**, 739–745. https://doi.org/10.1093/nsr/nwz035.

Jiang, L., Hua, Y., Hu, G.-L. & Hua, B.-Z. (2019b) Habitat divergence shapes the morphological diversity of larval insects: insights from scorpionflies. *Scientific Reports*, **9**, 12708. https://doi.org/10.1038/s41598-019-49211-z.

Krzemiński, W. & Soszyńska-Maj, A. (2012) A new genus and species of scorpionfly (Mecoptera) from Baltic amber, with an unusually developed postnotal organ. *Systematic Entomology*, **37**, 223–228. https://doi.org/10.1111/j.1365-3113.2011.00602.x.

Latreille, P.A. (1802) Histoire Naturelle, Générale et Particulière des Crustacés et des Insectes, *Tome Troisième*. De l'Imprimerie de F. Dufart, Paris, France.

Legg, D.A., Sutton, M.D. & Edgecombe, G.D. (2013) Arthropod fossil data increase congruence of morphological and molecular phylogenies. *Nature Communications*, **4**, 2485. https://doi.org/10.1038/ncomms3485.

Li, X., Hua, B.Z., Cai, L.J. & Huang, P.Y. (2007) Two new species of *Panorpa* (Mecoptera: Panorpidae) from Shaanxi, China with notes on their biology. *Zootaxa*, **1542**, 59–67. https://doi.org/10.11646/zootaxa.1542.1.5.

Lieftinck, M.A. (1936) Studies in Oriental Mecoptera. I: the genus *Leptopanorpa* in Malaysia. *Treubia*, **15**, 271–320.

Lin, X.-D., Shih, C.-K., Li, S. & Ren, D. (2019) Mecoptera – Scorpionflies and hangingflies. *Rhythms of Insect Evolution: Evidence from the Jurassic and Cretaceous in Northern China*, First edn (ed. by D. Ren, C.-K. Shih, T.-P. Gao, Y.-J. Wang and Y.-Z. Yao), pp. 555–595. John Wiley & Sons, Hoboken, New Jersey.

Ma, N. & Hua, B.-Z. (2011) *Furcatopanorpa*, a new genus of Panorpidae (Mecoptera) from China. *Journal of Natural History*, **45**, 2251–2261. https://doi.org/10.1080/00222933.2011.595517.

Ma, N., Cai, L.-J. & Hua, B.-Z. (2009) Comparative morphology of the eggs in some Panorpidae (Mecoptera) and their systematic implication. *Systematics and Biodiversity*, **7**, 403–417. https://doi.org/10.1017/S1477200009990107.

Ma, N., Zhong, W., Gao, Q.-H. & Hua, B.-Z. (2012) Female genital plate diversity and phylogenetic analyses of east Asian Panorpidae (Mecoptera). *Systematics and Biodiversity*, **10**, 159–178. https://doi.org/10.1080/14772000.2012.683459.

MacLachlan, R. (1875) A sketch of our present knowledge of the Neuropterous fauna of Japan (excluding Odonata and Trichoptera). *Transactions of the Royal Entomological Society of London*, **23**, 167–190.

Maddison, W.P. & Maddison, D.R. (2019) Mesquite: a modular system for evolutionary analysis. Version 3.61 [WWW document]. URL http://mesquiteproject.org [accessed on 26 December 2019].

Martynova, O.M. (1957) Mecoptera of the USSR. II. Family Panorpidae. *Entomologischeskoe Obozreni*, **36**, 721–747.

Meusemann, K., Trautwein, M., Friedrich F., Beutel, R.G., Wiegmann, B.M., Donath, A., *et al.* 2020. Are fleas highly modified Mecoptera? Phylogenetic resolution of Antliophora (Insecta: Holometabola). *BioRxiv*, https://doi.org/10.1101/2020.11.19.390666.

Miao, Y., Na, M. & Hua, B.-Z. (2017) Cytotaxonomy and molecular phylogeny of the genus *Cerapanorpa* Gao, Ma & Hua, 2016 (Mecoptera: Panorpidae). *Scientific Reports*, **7**, 4493. https://doi.org/10.1038/s41598-017-04926-9.

Miao, Y., Wang, J.-S. & Hua, B.-Z. (2019) Molecular phylogeny of the scorpionflies Panorpidae (Insecta: Mecoptera) and chromosomal evolution. *Cladistics*, **35**, 385–400. https://doi.org/10.1111/cla.12357.

Mickoleit, G. (1975) Die Genital- und Postgenitalsegmente der Mecoptera-Weibchen (Insecta, Holometabola) I. Das Exoskelet. *Zeitschrift für Morphologie der Tiere*, **80**, 97–135.

Mickoleit, G. (1976) Die Genital- und Postgenitalsegmente der Mecoptera-Weibchen (Insecta, Holometabola) II. Das Dach der Geritalkammer. *Zoomorphologie*, **85**, 133–156.

Mickoleit, G. (1978) Die phylogenetischen Beziehungen der Schnabelfliegen-Familien aufgrund morphologischer Ausprägungen der weiblichen Genital- und Postgenitalsegmente (Mecoptera). *Entomologica Germanica*, **4**, 258–271.

Mickoleit, G. (2008) Die Sperma-Auspreßvorrichtung der Nannochoristidae (Insecta: Mecoptera). *Entomologia Generalis*, **31**, 193–226. https://doi.org/10.1127/entom.gen/31/2008/193.

Mikkola, K., Lafontaine, J.D. & Kononenko, V.S. (1991) Zoogeography of the Holarctic species of the Noctuidae (Lepidoptera): importance of the Beringian refuge. *Entomologica Fennica*, **2**, 157–173.

Minh, B.Q., Schmidt, H.A., Chernomor, O., Schrempf, D., Woodhams, M.D., von Haeseler, A. & Lanfear, R. (2020) IQ-TREE 2: new models and efficient methods for phylogenetic inference in the genomic era. *Molecular Biology and Evolution*, **37**, 1530–1534. https://doi.org/10.1093/molbev/msaa015.

Misof, B., Erpenbeck, D. & Sauer, K.P. (2000) Mitochondrial gene fragments suggest paraphyly of the genus *Panorpa* (Mecoptera, Panorpidae). *Molecular Phylogenetics and Evolution*, **17**, 76–84. https://doi.org/10.1006/mpev.2000.0817.

Misof, B., Liu, S., Meusemann, K., Peters, R. S., Donath, A., Mayer, C., Frandsen, P. B., Ware, J., Flouri, T., Beutel, R. G., Niehuis, O., Petersen, M., Izquierdo-Carrasco, F., Wappler, T., Rust, J., Aberer, A. J., Aspock, U., Aspock, H., Bartel, D., Blanke, A., Berger, S., Bohm, A., Buckley, T. R., Calcott, B., Chen, J., Friedrich, F., Fukui, M., Fujita, M., Greve, C., Grobe, P., Gu, S., Huang, Y., Jermiin, L. S., Kawahara, A. Y., Krogmann, L., Kubiak, M., Lanfear, R., Letsch, H., Li, Y., Li, Z., Li, J., Lu, H., Machida, R., Mashimo, Y., Kapli, P., McKenna, D. D., Meng, G., Nakagaki, Y., Navarrete-Heredia, J. L., Ott, M., Ou, Y., Pass, G., Podsiadlowski, L., Pohl, H., von Reumont, B. M., Schutte, K., Sekiya, K., Shimizu, S., Slipinski, A., Stamatakis, A., Song, W., Su, X., Szucsich, N. U., Tan, M., Tan, X., Tang, M., Tang, J., Timelthaler, G., Tomizuka, S., Trautwein, M., Tong, X., Uchifune, T., Walzl, M. G., Wiegmann, B. M., Wilbrandt, J., Wipfler, B., Wong, T. K. F., Wu, Q., Wu, G.,

Xie, Y., Yang, S., Yang, Q., Yeates, D. K., Yoshizawa, K., Zhang, Q., Zhang, R., Zhang, W., Zhang, Y., Zhao, J., Zhou, C., Zhou, L., Ziesmann, T., Zou, S., Li, Y., Xu, X., Zhang, Y., Yang, H., Wang, J., Wang, J., Kjer, K. M., & (2014) Phylogenomics resolves the timing and pattern of insect evolution. *Science*, **346** , 763–767. http://dx.doi.org/10.1126/science.1257570.

Miyaké, T. (1908) A list of Panorpidae of Japan, with descriptions of ten new species. *Bulletin of the College of Agriculture, Tokyo Imperial University*, **8**, 1–12.

Miyaké, T. (1910) A further contribution towards the knowledge of the Panorpidae of Japan. *Journal of the College of Agriculture of the Imperial University of Tokyo*, **2**, 183–205.

Miyaké, T. (1911) A synonymic list of the Panorpidae of Japan, with corrections to my former paper, and description of new species. *Entomologiste*, **44**, 90–94.

Miyaké, T. (1913) Studies of the Mecoptera of Japan. *Journal of the College of Agriculture, Imperial University of Tokyo*, **4**, 265–400.

Miyamoto, S. (1977) Geographical forms in the Leucoptera-group of the genus *Panorpa* Linnaeus (1) (Insecta: Mecoptera). *Journal of Chikushi Jogakuen Junior College*, **12**, 91–102.

Miyamoto, S. (1978) Geographical forms in the Leucoptera-group of the genus *Panorpa* Linnaeus (2) (Insecta: Mecoptera). *Journal of Chikushi Jogakuen Junior College*, **13**, 37–44.

Miyamoto, S. (1984) New species and subspecies of the Mecoptera in Japan (Insecta). *Journal of Chikushi Jogakuen Junior College*, **19**, 1–16.

Miyamoto, S. (1985) New and little-known Panorpidae of Japan. *Journal of Chikushi Jogakuen Junior College*, **20**, 23–31.

Miyamoto, S. & Makihara, H. (1979) A new species of the genus *Neopanorpa* Weele from the Nansei Islands (Mecoptera). *Esakia*, **14**, 57–60.

Miyamoto, S. & Nakamura, T. (2008) Mecoptera. *Iconographia Insectorum Japonicorum Colore Naturali Edita. III* (ed. by Y. Hirashima and K. Morimoto), pp. 229–233. Hokiryukan, Tokyo.

Myers, N., Mittermeier, R.A., Mittermeier, C.G., Da Fonseca, G.A. & Kent, J. (2000) Biodiversity hotspots for conservation priorities. *Nature*, **403**, 853–858. https://doi.org/10.1038/35002501.

Nakamura, T. (2009) A redescription of *Panorpa amamiensis* and descriptions of its closely allied two new species from the Ryukyu Islands, Japan (Mecoptera, Panorpidae). *Japanese Journal of Systematic Entomology*, **15**, 333–342.

Nakamura, T., Bicha, W. & Saigusa, T. (2019) Systematic study of the short-faced scorpionfly genus *Panorpodes* M'Lachlan with descriptions of seven new species (Mecoptera: Panorpodidae). *Japanese Journal of Systematic Entomology*, **25**, 19–38.

Nixon, K.C. (2002) *Winclada ver. 1.0000*. Nixon, Ithaca, New York.

Novokshonov, V.G. (2004) The first Mecopteroids (Insecta: Papilionidea = Mecopteroidea) and the origin of scorpionflies (Panorpida = Mecoptera), with description of a legless eruciform larva from the lower Permian of Tshekarda. *Paleontological Journal*, **38**(Supplement 2), 204–213.

Penny, N.D. & Byers, G.W. (1979) A check-list of the Mecoptera of the world. *Acta Amazonica*, **9**, 365–388. https://doi.org/10.1590/1809-43921979092365.

Rust, M.K. & Byers, G.W. (1976) The Mecoptera of India and adjacent regions. *University of Kansas Science Bulletin*, **51**, 19–90.

Sanmartin, I., Enghoff, H. & Ronquist, F. (2001) Patterns of animal dispersal, vicariance and diversification in the Holarctic. *Biological Journal of the Linnean Society*, **73**, 345–390.

Santos, B.F., Payne, A., Pickett, K.M. & Carpenter, J.M. (2015) Phylogeny and historical biogeography of the paper wasp genus *Polistes* (hymenoptera: Vespidae): implications for the overwintering hypothesis of social evolution. *Cladistics*, **31**, 535–549. https://doi.org/10.1111/cla.12103.

Scudder, S.H. (1890) The tertiary insects of North America. *Report of the United States Geological Survey of the Territories*, **8**, 1–734.

Somma, L.A. (2011) The correct publication date for mecopteran insects (Choristidae, Bittacidae, and Panorpidae) described by John Obadiah Westwood, resurrecting *Panorpa confusa* Westwood, 1841, the confused scorpionfly. *Zootaxa*, **3121**, 61–65. https://doi.org/10.11646/zootaxa.3121.1.2.

Soszyńska-Maj, A., Krzemiński, W., Kopeć, K., Cao, Y.-Z. & Ren, D. (2020) New middle Jurassic fossils shed light on the relationship of recent Panorpoidea (Insecta, Mecoptera). *Historical Biology*, **32**, 1081–1097. https://doi.org/10.1080/08912963.2018.1564747.

Statz, G. (1936) Ueber neue funde von Neuropteren, Panorpaten und Trichopteren aus den Tertiären schiesfern von Rott am Siebengebirge. *Decheniana*, **93**, 208–255.

Tihelka, E., Giacomelli, M., Huang, D.-Y., Pisani, D., Donoghue, P.C.J. & Cai, C.-Y. (2020) Fleas are parasitic scorpionflies. *Palaeoentomology*, **3**, 641–653. https://doi.org/10.11646/palaeoentomology.3.6.16.

Tojo, K., Sekine, K., Takenaka, M., Isaka, Y., Komaki, S., Suzuki, T. & Schoville, S.D. (2017) Species diversity of insects in Japan: their origins and diversification processes. *Entomological Science*, **20**, 357–381. https://doi.org/10.1111/ens.12261.

Vila, R., Bell, C.D., Macniven, R. *et al.* (2011) Phylogeny and palaeoecology of *Polyommatus* blue butterflies show Beringia was a climate-regulated gateway to the New World. *Proceedings of the Royal Society B-Biological Science*, **278**, 2737–2744. https://doi.org/10.1098/rspb.2010.2213.

Wang, J.-S. & Hua, B.-Z. (2017) An annotated checklist of the Chinese Mecoptera with description of male *Panorpa guttata* Navás, 1908. *Entomotaxonomia*, **39**, 24–42. https://doi.org/10.11680/entomotax.2017003.

Wang, J.-S. & Hua, B.-Z. (2018) *A Color Atlas of the Chinese Mecoptera*. Henan Science and Technology Press, Zhengzhou.

Wang, J.-S. & Hua, B.-Z. (2019a) *Megapanorpa*, a new genus with a single anal horn in males from Oriental China (Mecoptera: Panorpidae). *Entomological Science*, **22**, 64–79. https://doi.org/10.1111/ens.12336.

Wang, J.-S. & Hua, B.-Z. (2019b) Taxonomy of the genus *Neopanorpa* van der Weele, 1909 (Mecoptera, Panorpidae) from the Oriental Region, with the description of two new species. *European Journal of Taxonomy*, **543**, 1–17. https://doi.org/10.5852/ejt.2019.543.

Wang, J.-S. & Hua, B.-Z. (2020) Taxonomic revision and phylogenetic analysis of the enigmatic scorpionfly genus *Leptopanorpa* MacLachlan (Mecoptera: Panorpidae). *Journal of Zoological Systematics and Evolutionary Research*, **58**, 900–928. https://doi.org/10.1111/jzs.12363.

Wang, J.-S., Gao, X.-T. & Hua, B.-Z. (2019) Two new species of the genus *Panorpa* (Mecoptera, Panorpidae) from eastern China and a new synonym. *ZooKeys*, **874**, 149–164. https://doi.org/10.3897/zookeys.874.36314.

van der Weele, H.W. (1909) Mecoptera and Planipennia of Insulinde. *Notes from the Leyden Museum*, **31**, 1–100.

Whiting, M.F. (2002) Mecoptera is paraphyletic: multiple genes and phylogeny of Mecoptera and Siphonaptera. *Zoologica Scripta*, **31**, 93–104. https://doi.org/10.1046/j.0300-3256.2001.00095.x.

Willmann, R. (1976) *Panorpa rhenana* nom. nov., eine Skorpionfliege aus dem Oligozan (Insecta, Mecoptera). *Neues Jahrbuch für Geologie und Paläontologie Monatshefte*, **1976**, 574–576.

Willmann, R. (1977) Zur Phylogenie der Panorpiden Europas (Insecta, Mecoptera). *Zeitschrift für Zoologische Systematik und Evolutionsforschung*, **15**, 208–231.

Willmann, R. (1983) Widersprüchliche Rekonstruktionen der Phylogenese am Beispiel der Ordnung Mecoptera (Schnabelfliegen; Insecta: Holometabola). *Paläontologische Zeitschrift*, **57**, 285–308.

Willmann, R. (1987) The phylogenetic system of the Mecoptera. *Systematic Entomology*, **12**, 519–524.

Willmann, R. (1989) Evolution und phylogenetisches system der Mecoptera (Insecta: Holometabola). *Abhandlungen der Senckenbergischen Naturforschenden Gesellschaft*, **554**, 1–153.

Zakharov, Y.D., Shigeta, Y., Popov, A.M., Velivetskaya, T.A. & Afanasyeva, T.B. (2011) Cretaceous climatic oscillations in the Bering area (Alaska and Koryak upland): isotopic and palaeontological evidence. *Sedimentary Geology*, **235**, 122–131. https://doi.org/10.1016/j.sedgeo.2010.03.012.

Zhong, W. & Hua, B.-Z. (2013) *Dicerapanorpa*, a new genus of east Asian Panorpidae (Insecta: Mecoptera: Panorpidae) with descriptions of two new species. *Journal of Natural History*, **47**, 1019–1046. https://doi.org/10.1080/00222933.2012.752540.

Accepted 22 February 2021